GREEN SYNTHESIS OF SILVER NANOPARTICLES FROM *DEBREGEASIA LONGIFOLIA* (BURM. F.) WEDD. LEAF EXTRACT AND THEIR ANTIOXIDANT, ANTIBACTERIAL AND ANTIDIABETIC APPLICATIONS

MUSTAFA, M.[1] – NAZIR, N.[1*] – HUSSAIN, J.[1] – AZAM, A.[1] – KHAN, J.[2] – NISAR, M.[3] – AZIZ, T.[4*] – AL-ASMARI, F.[5] – ALWETHAYNANI, M. S.[6] – AL JOUFI, F.[7] – NAHARI, A. M.[8] – ALYAMANI, S. A.[9]

[1]*Department of Biochemistry, University of Malakand, Chakdara, Dir Lower 18800, Pakistan*

[2]*Department of Pharmacy, University of Malakand, Chakdara, Dir Lower 18800, Pakistan*

[3]*Department of Botany, University of Malakand, Chakdara, Dir Lower 18800, Pakistan*

[4]*Laboratory of Animal Health, Food Hygiene and Quality, University of Ioannina, Arta 47132, Greece*

[5]*Department of Food and Nutrition Sciences, College of Agricultural and Food Sciences, King Faisal University, Al Ahsa, Saudi Arabia*

[6]*Department of Clinical Laboratory Sciences, College of Applied Medical Sciences, Shaqra University, Alquwayiyah, Riyadh, Saudi Arabia*

[7]*Department of Pharmacology, College of Pharmacy, Jouf University, 72341 Aljouf, Saudi Arabia*

[8]*University of Jeddah, College of Science, Department of Biological Sciences, 21493 Jeddah, Saudi Arabia*

[9]*Department of Biology, Preparatory Year Program, Batterjee Medical College, Jeddah 21442, Saudi Arabia*

[*]*Corresponding authors*
e-mail: nasheen.nazir@uom.edu.pk, iwockd@gmail.com

(Received 31st Jan 2025; accepted 13th May 2025)

Abstract. This study focused on synthesising silver nanoparticles (AgNPs) using aqueous leaf extract of *Debregeasia longifolia* and compared their properties with methanolic extract (Met-Ext-D.L) for antioxidants, antibacterial, and antidiabetic potential. Gas chromatography-mass spectrometry (GC-MS) identified 50 bioactive compounds in Met-Ext-D.L. The formation of AgNPs was confirmed by UV-visible spectroscopy, showing an SPR peak in 300-400 nm range. Fourier-transform infrared spectroscopy (FTIR) showed 4 peaks (3276.33, 2094.76, 1632.57, and 421.19 cm^{-1}), indicating the presence of functional groups. X-ray diffraction (XRD) confirmed the cubic crystalline structure of AgNPs, and energy-dispersive X-ray spectroscopy (EDX) identified silver as a major element (48.77%). Scanning electron microscopy (SEM) showed spherical AgNPs, ranging from 10-100 nm in size. Both Met-Ext-D.L and AgNPs-D.L showed significant free radicals scavenging activity, with AgNPs showing the highest activity (88% at 1000 µg/mL, IC_{50} = 80 µg/mL). They also showed good antibacterial activity against *Enterococcus faecalis*, *Klebsiella pneumoniae*, and *Pseudomonas aeruginosa* in Kirby-Bauer disc diffusion assay. They were also effective in inhibiting α-amylase and α-glucosidase enzymes, with AgNPs showing the highest % inhibitory potential than Met-Ext-D.L. These findings highlight the potential of AgNPs-D.L as effective agents in managing oxidative stress, bacterial infections, and diabetes, thereby supporting their use in developing new therapeutic formulations.

http://www.aloki.hu ● ISSN 1589 1623 (Print) ● ISSN 1785 0037 (Online)
DOI: http://dx.doi.org/10.15666/aeer/2304_67876815

Keywords: *D. longifolia, AgNPs, nanoparticle biosynthesis, nanoparticle characterisation, GC-MS, UV-visible, FTIR, XRD, EDX, SEM, DPPH scavenging, plant-based synthesis, nanomedicine*

Introduction

Nanotechnology is an interdisciplinary branch of science and engineering that integrates chemistry, biology, material science, and physics for developing, analysing, and using materials and devices at the nanoscale, which is around one billionth of a meter (Dhale and Sharma, 2023). The growing interest in nanoparticles is due to their numerous applications across various technologies and special properties, such as a high ratio of surface area to volume, which enhances their reactivity and enables them to penetrate cell membranes, thereby boosting their biochemical activity. These nanoparticles are increasingly applied in medical treatments, industrial operations, and everyday products like clothes and cosmetics. Nanoparticles, or NPs, are atomic or molecular structures with a size between 1 and 100 nanometres in at least one dimension. They have modified electromagnetic and catalytic characteristics, reduced melting points, increased light absorption, specific heat, electrical resistivity, plasticity, diffusivity, and tensile strength. NPs have applications in electrical logic, memory systems, sensors, biosensing, transistors, optics, electrometers, bactericidal activities, medication administration, imaging, nanocomposites, filters, and malignancies (Altammar, 2023).

In general, inorganic nanoparticles have a variety of flexible characteristics that make them ideal for cellular transportation. These characteristics contain their broad availability, rich functionality, high biological compatibility, potential for targeted delivery (e.g., specifically killing cancer cells while protecting healthy tissues), as well as controlled release of the drugs they carry. Inorganic nanoparticles are usually made of metals or metal oxides. One such type of inorganic nanoparticle is AgNPs, which are known for their strong antimicrobial properties. They are without a doubt the most widely utilised nanoparticles, finding application in sunblock creams, for water disinfection, and as antibacterial agents in the textile industry (Rai et al., 2009).

Different techniques are used for synthesising NPs, including chemical, physical, and biological methods. The physical approach uses heating, mechanical, electrical, or radiation techniques with high energies to eliminate, vaporise, or condense substances for synthesising NPs. These methods, primarily using a top-down strategy, offer the advantage of generating uniform, monodisperse NPs without polluting the solvent. Simultaneously, physical processes exhibit reduced efficiency because of the substantial quantities of waste produced during synthesis. Common physical methods for producing nanoparticles include laser ablation, inert gas condensation, melt mixing, flash spray pyrolysis, high-energy ball milling, physical vapour deposition, and laser pyrolysis. Similarly, many chemical processes are also used for synthesising nanoparticles, of which some of the most widely used methods are the hydrothermal synthesis, microemulsion technique, sol-gel method, vapour phase chemical synthesis, polyol synthesis, and plasma accelerated chemical vapour deposition technique (Dhand et al., 2015). The main drawback of the chemical and physical methods used in the production of NPs is their high expense, utilisation of hazardous and toxic compounds, and the possible hazards they provide to both the environment and biological systems (Bhardwaj et al., 2020).

The biological method provides an environmentally friendly alternative to chemical and physical techniques for producing NPs. It is also known as green synthesis which is a bottom-up strategy used to synthesise AgNPs by gathering and combining gaseous or

http://www.aloki.hu ● ISSN 1589 1623 (Print) ● ISSN 1785 0037 (Online)
DOI: http://dx.doi.org/10.15666/aeer/2304_67876815

liquid molecules or atoms. This technique uses living organisms like plants, bacteria, moulds, actinobacteria, algae, yeasts, and their derivatives to produce metallic nanoparticles with diverse characteristics, including different forms, sizes, compositions, and physicochemical qualities (Nadaroglu et al., 2017). Conventional chemical and physical techniques often include reducing agents and stabilising agents, which have the potential to be dangerous to the environment and cells. These materials are found in the organisms employed in biogenic synthesis. Bacteria are selected because of their fast proliferation, cost-effective culture expenses, and manageable regulation of growth conditions. Actinobacteria exhibit resistance to harmful heavy metals and can synthesise nanoparticles that have antibacterial, antifungal, anticancer, antioxidant, and catalytic properties. Synthesis may be carried out either outside or within the cell, utilising enzymes, using easily cultivated and rapidly reproducing eukaryotic yeasts and moulds. Algae, which are eukaryotic photosynthetic organisms found in water, can convert metallic ions into nanoparticles via the use of carbohydrates, pigments, nucleic acids, fats, proteins, and secondary metabolites. Plants possess significant capabilities for detoxifying, reducing, and accumulating metals, as well as synthesising metallic nanoparticles with diverse morphological features (Hussain et al., 2016).

Silver is used for the production of green nanoparticles because of its many qualities, including its ability to fight against microorganisms such as bacteria, viruses, and fungi, which are very beneficial in medical applications such as wound healing and coatings. The key process involved in the synthesis of AgNPs is the reduction/oxidation reaction in which the bioactive compounds in the plant extract reduce silver ions (Ag^{+}) into AgNPs (Ag^{0}). Because of its antibacterial properties, Nanosilver, a substance utilised in nanoformulation, has been employed in a variety of consumer and medicinal products. It has been used in filtration systems for cleaning drinking water and swimming pool water. AgNPs are made up of 15–20,000 silver atoms and are typically smaller than 100 nm. The production of these nanostructures might take the form of tubes, wires, multifactes, or films. AgNPs have different physicochemical characteristics and biological effects in comparison to conventional metals, owing to their greater surface area per unit mass. The main reason for the development of goods containing nanosilver is its strong antibacterial qualities. These features allow for a variety of uses, including food packaging, electronics, water disinfectants, room sprays, odour-resistant textiles, and cosmetics (Ramya and Subapriya, 2012).

The *Urticaceae* family, which comprises 59 accepted genera and 600 species, belongs to the major group of angiosperms. It is commonly known as the nettle family and is native to tropical, subtropical, and temperate regions (The World Flora Online, 2024). *Debregeasia Gaudich*. is a recognised genus within the *Urticaceae* family. It was first described by Gaudich in 1844-52. Other botanists, like Boys, Benth & Hook.f, and Hutch, also talked about it in their works. The genus *Debregeasia Gaudich.* encompasses a total of nine recognised species and has a native range extending from northeast tropical Africa to the tropical and subtropical regions of Asia, reaching as far as the southwestern Pacific (The World Flora Online, 2024).

Debregeasia longifolia belongs to the genus *Debregeasia* and family *Urticaceae,* which was described for the first time in 1869 by the botanist *Alphonse Louis Pierre Pyramus de Candolle*. The plant is distributed across a wide geographic area, stretching from China to Tropical Asia and even Vanuatu in the Southwestern Pacific. It is a shrub or tree that grows efficiently in moist environments (Plants of the World Online | Kew Science). In Khyber Pakhtunkhwa, Pakistan, it is commonly referred to as "*Khar-Wala*."

http://www.aloki.hu ● ISSN 1589 1623 (Print) ● ISSN 1785 0037 (Online)
DOI: http://dx.doi.org/10.15666/aeer/2304_67876815

while in English it is known as "*Wild Rhea*,". Its nomenclature varies across languages and countries, showing the widespread presence and cultural significance of this species across different communities and regions (India Biodiversity Portal).

Previous studies have identified an abundance of phytochemicals in different parts of *D. longifolia* that are responsible for different pharmacological effects. Various compounds were found by ultra-high-performance liquid chromatography (UHPLC) of *D. longifolia* leaves. These include chlorogenic acid (6.25), catechin (0.39), caffeic acid (3.09), coumaric acid (0.29), gallic acid (0.02), rutin (46.91), umbelliferone (0.8), ellagic acid (0.93), epicatechin (1.99), kaempferol (16.07), and total polyphenols (76.79 µg/g dry weight) (Kumar et al., 2015). Similarly, *D. longifolia* also contains phenols, flavonols, alkaloids, tannins, saponins, vitamin C, vitamin E, carotenoids, and flavonoids (Tapan and Kaushik, 2015; Devi, 2016; Devi et al., 2016; Radhamani and Britto, 2016). The antioxidant capacity of *D. longifolia* has been measured using different assays like 1,1-diphenyl-2-picryl hydrazyl (DPPH) and 2,2′-azino-bis(3-ethylbenzothiazoline-6-sulphonic acid (ABTS) (Tapan and Kaushik, 2015; Devi, 2016; Radhamani and Britto, 2016). The ethanolic extract of *D. longifolia* demonstrated strong antimicrobial properties in an agar diffusion assay and micro broth dilution method against various microorganisms (Mariani et al., 2014). *D. longifolia* holds significant traditional importance. Its bark provides fine fibre utilised in clothing stitching. Among the Sumi tribe in Nagaland, both the fruits and bark serve as ingredients for shampooing and aiding digestion. Tender leaves are ingested during dysentery, while crushed leaves are applied topically to alleviate arthritis. In Azad Kashmir, the leaves function as veterinary medicine for diarrhoea and flatulence, and they are also utilised to treat scabies in humans and animals. The bark is utilised as shampoo, and the fruits aid in digestion. Indigenous communities in Indonesia utilise it for construction and fuel. In traditional Batak Karo cuisine, its leaves are employed for digestive therapy. This versatile plant is esteemed for its efficacy in treating various ailments, including diabetes, skin conditions, and bone fractures, and it is also utilised in rope making and as fodder (Mahmoud, 2019).

The current research aimed to utilise these advantageous characteristics of *D. longifolia* to produce AgNPs with improved efficacy. In this study, the Aq-Ext-D.L was used to synthesise AgNPs, which were then characterised by UV-visible spectrophotometry, FTIR spectroscopy, XRD analysis, SEM analysis, and EDX spectroscopy. The chemical profiling of Met-Ext was accomplished by GC-MS analysis. The Met-Ext and synthesised AgNPs were evaluated for different biological activities to assess their potential as antioxidant, antibacterial, and antidiabetic agents.

Materials and methods

Materials

All the chemicals used in this study were of analytical grade. The chemicals utilised in this research included silver nitrate ($AgNO_3$) procured from Merck (Germany), DPPH obtained from Sigma-Aldrich (USA), and methanol supplied by Merck (Germany). Additionally, imipenem discs, nutrient agar, and an antidiabetic kit comprising Type I α-Glucosidase, Type VI α-Amylase, and PNPG (p-Nitrophenyl-α-D-glucopyranoside) were utilised. Potassium phosphate buffer was purchased from Sigma-Aldrich (Paris, France), while 3,5-dinitrosalicylic acid and ascorbic acid were acquired from Sigma-Aldrich (USA). All aqueous solutions were produced using distilled water. All glasswares were washed with distilled water and dried before use.

http://www.aloki.hu ● ISSN 1589 1623 (Print) ● ISSN 1785 0037 (Online)
DOI: http://dx.doi.org/10.15666/aeer/2304_67876815

Sample collection and pre-treatment

The leaves of *D. longifolia* were acquired from the district Dir of Khyber Pakhtunkhwa. The first specimens were verified by an expert in the field of taxonomy from the Botany Department, University of Malakand, KPK, Pakistan. Dust and other contaminants were cleaned from the surface of leaves by washing them first with normal water and then with distilled water (DW). After washing, the leaves were placed on clean white paper in the shade to dry for nearly 20 days. The purpose of keeping in the shade is to avoid any variation in structure. The dried leaves were then pulverised with an electric grinder and stored in a refrigerator for future use.

Preparation of methanolic extract of D. longifolia leaves

The method used for preparing the methanolic extract (Met-Ext) was based on the already established procedure by Nazir et al. (2018). The powdered leaves of *D. longifolia* were macerated in 80% methanol for nearly 3 days (72 h) while being constantly shaken. After 14 days, the solution was passed through the Whatman No. 1 filter paper. The undissolved materials and other debris were removed, and the filtrate was collected in a beaker and shifted into a round-bottom flask of the rotary evaporator (SCI100-Pro; SCILOGEX, USA), which helped to separate the solvent and concentrate the resulting extract under reduced pressure at 40 ^{0}C using a vacuum pump. After this, the remaining water content was removed by further drying at 60 °C using a water bath. This resulted in the formation of a thick paste, which was termed as crude methanolic extract of *D. longifolia* (Met-Ext-D.L). Such extract was then stored in a refrigerator (HF3-700S, USA) at 30 °C.

GC-MS profiling of components in methanolic extract (Met-Ext)

The Met-Ext-D.L was subjected to a gas chromatography (GC) analysis using a Shimadzu GC 17A-QP5050A gas chromatograph. The oven was set to heat up at a rate of 10 °C per minute and maintain a temperature of 290 °C. Helium gas was used to transport the sample through the system, and it flowed at a rate of one millilitre per minute. A split sampling method was employed to introduce the sample into the system at a 1:10 ratio. The retention index of each component was checked against known data from research or actual compounds to verify their identities. The mass spectrum was examined using the NIST database, which includes more than 62,000 different spectral patterns for reference. The spectra of the recognised and unknown components from the NIST collection were compared.

Synthesis of AgNPs

Aqueous extract preparation from D. longifolia leaves

AgNPs were prepared by mixing the aqueous extract of *D. longifolia* leaves (Aq-Ext-D.L) with 1 mM silver nitrate ($AgNO_3$) solution. The Aq-Ext-D.L was prepared by taking 20 g of powdered leaves in 200 ml of DW (10:1 w:v) and heating at 60 °C for 30 minutes. After heating, the mixture was allowed to cool down and then filtered using a velvet cloth and Whatman filter paper No.1 to separate the crude components from the liquid form. The solid residue was discarded, and the filtrate (aqueous extract) was stored for further use.

http://www.aloki.hu ● ISSN 1589 1623 (Print) ● ISSN 1785 0037 (Online)
DOI: http://dx.doi.org/10.15666/aeer/2304_67876815

The $AgNO_3$ solution was prepared by dissolving 0.068 g of $AgNO_3$ in 400 ml of DW. The same amount of Aq-Ext-D.L (1 ml) was combined with different amounts of 1 mM $AgNO_3$ solution, i.e., 1:1, 1:2, 1:3, 1:4, and 1:5, respectively. The reaction mixtures were then continuously agitated for 4 hours in a shaker. During this time, the colourless solution turned dark brown, indicating the formation of AgNPs. This colour shift was a confirmation of the chemical reaction occurring between the silver nitrate and the components present in the plant extract, resulting in the synthesis of AgNPs. The optimum ratio for the synthesis of AgNPs was determined using UV-visible spectroscopy analysis. The results indicated that a ratio of 1:3 of Aq-Ext-D.L to $AgNO_3$ solution was the most appropriate. Therefore, further synthesis was performed using this ratio.

To obtain powdered AgNPs, the reaction mixture was centrifuged at 14,000 revolutions per minute (rpm) for 20 minutes. The liquid was removed, and the pellet was washed three times with DW. Ultimately, the AgNPs pellet was carefully transferred from the Eppendorf tubes to a Falcon tube using a spatula spoon and placed in an incubator to remove the remaining liquid.

Methods of characterization

UV-visible spectroscopy

This method is used for initial confirmation of NP synthesis and its stability. It is considered a very reliable and useful method for characterizing NPs. Due to the exceptional optical properties of AgNPs, they interact with particular light wavelengths. Moreover, this method is rapid, simple, sensitive, easy, and selective for different NPs. For measurement, it requires a very short time and also does not need any final calibration (Patil and Chougale, 2021).

The reaction mixture of AgNPs was diluted to the appropriate concentration by adding DW so that it fell within the range of the UV-visible spectrophotometer (UV-1800 series). The diluted reaction mixture was added to a cuvette and placed in the sample holder. Another cuvette filled with DW was placed in the reference holder. The wavelength range was specified from 200 nm to 800 nm, and a fast scan of the sample was performed. The absorbance was recorded and presented in the form of a graph.

XRD

This technique is used to identify the nature of crystallinity at the atomic level and is, therefore, one of the primary used methods. It is a non-destructive method that can characterise materials of both organic and inorganic nature. This technique usually conducts quantitative analysis, measures phase identification, and is also involved in the determination of structure imperfections in samples from different fields, including geography, environmental, forensic, polymer, and pharmaceutical sciences. XRD works on the principle of Bragg's law (Patil and Chougale, 2021). AgNPs were examined with the help of an X-ray diffractometer (JDX-3532 JEOL, Japan), which gave us the respective XRD pattern from which information regarding the crystalline structure was obtained by comparing with standard reference patterns.

FTIR

FTIR is used to identify different functional groups present in the sample and to show the involvement of biomolecules in the production of NPs (Patil and Chougale, 2021).

http://www.aloki.hu ● ISSN 1589 1623 (Print) ● ISSN 1785 0037 (Online)
DOI: http://dx.doi.org/10.15666/aeer/2304_67876815

Synthesised AgNPs were analysed with the help of Cary630 (Agilent Technologies, USA) to identify the various types of functional groups present on their surface.

EDX

EDX performs the chemical analysis of the synthesised AgNPs and establishes their elemental composition to verify whether AgNPs have been synthesised or not. The EDX technique examines how the sample interacts and responds to the stimulation of the incident X-rays. The identification of elements is based on the fundamental concept that each element possesses a unique and distinguishable atomic structure, which is manifested in a different pattern of peaks on its electromagnetic emission spectrum (Yang, 2021). EDX analysis of the synthesised AgNPs-D.L was performed by an EDX-7000 (Shimadzu, Japan). The powdered AgNPs were placed in a suitable holder and inserted into the sample chamber of the EDX machine. The specific EDX patterns were acquired using SEM.

SEM

A surface imaging method, SEM has the potential to resolve the size, shapes, distribution, and morphology of different particles fabricated at nano and micro scales. Through the SEM technique, the particle morphology can be investigated, thereby plotting a histogram from the image either via manual counting/measuring or employing appropriate software (Patil and Chougale, 2021). SEM and EDX, when combined, can examine the morphology of Ag powder and can analyse chemical composition. SEM analysis was performed at Centralized Resource Laboratory (CRL) - University of Peshawar, Peshawar, KPK using a JSM5910 (JEOL, Japan) scanning electron microscope.

Antioxidant activity

The antioxidant capacity of Met-Ext-D.L and AgNPs-D.L to neutralise DPPH free radicals was evaluated by the Brand-Williams test (Brand-Williams et al., 1995). DPPH solution was made by mixing 24 mg DPPH reagent in 100 mL of methanol. In addition, stock solutions (1 mg/mL) of Met-Ext in methanol and AgNPs in DW were prepared which were then diluted in their respective solvent to prepare samples of different concentrations ranging from 1000 to 62.5 µg/mL. For performing the assay, 0.1 mL was taken from each diluted sample and mixed with 3 mL of the DPPH solution. This combination allows for the interaction between the sample and the DPPH reagent to test for radical scavenging activity. After mixing, the samples were kept in an incubator for 30 minutes, which was set at a temperature of 25 °C. After this, the samples were checked at 517 nm using a UV-visible spectrophotometer. Ascorbic acid was utilised as a positive reference. The experiment was repeated thrice for each dilution, and the results were shown as Mean ± SEM. The DPPH scavenging potential was determined using the following formula:

$$\%\ DPPH\ Scavenging\ activity = \frac{absorbance\ of\ the\ standard\ -\ absorbance\ of\ the\ sample}{absorbance\ of\ the\ standard} \times 100 \quad \text{(Eq.1)}$$

http://www.aloki.hu ● ISSN 1589 1623 (Print) ● ISSN 1785 0037 (Online)
DOI: http://dx.doi.org/10.15666/aeer/2304_67876815

Antibacterial activity

The ability of Met-Ext-D.L and AgNPs-D.L to inhibit bacterial growth was examined by using the Kirby-Bauer disc diffusion assay, following the guidelines of the Clinical and Laboratory Standards Institute (CLSI, 2012). To prepare the inoculum, a few colonies of the tested microorganisms were dissolved in nutrient agar such that its turbidity became equivalent to 0.5 McFarland. This standard is known to contain approximately 1×10^8 colony-forming units (CFU/mL) of bacterial cells. The prepared inoculum was evenly swabbed across the surface of the media to ensure uniform distribution. 0.1 mg of each Met-Ext and AgNPs was dissolved in 1 ml of DW for testing against the bacteria. Sterile discs of 6 mm in diameter were soaked with 100 µL of these samples and placed on the inoculated agar plate. Distilled water-soaked discs were taken as a negative control, while the antibiotic discs of imipenem were used as a standard for comparison. The plates were then placed in an incubator and maintained at 37°C overnight, and were inspected the next day after 24 hours. Both Met-Ext-D.L and AgNPs-D.L showed visible zones of inhibition, which were measured in millimetres using a measuring scale. The activity was repeated three times, and the values were expressed as mean ± standard error of mean.

Inhibition of α-glucosidase activity

The experiment that was previously reported was used to evaluate the α-glucosidase inhibitory capability of Met-Ext-D.L and AgNPs-D.L, with some minor changes (Nazir et al., 2021). Various concentrations of Met-Ext-D.L and AgNPs-D.L were prepared by diluting their stock solutions. The concentrations ranged from 62.5 µg/mL to 1000 µg/mL. 50 µL of each sample was mixed with phosphate buffer (600 ul) and α-glucosidase (100 µL) to form a reaction mixture. Each reaction mixture was added with 5 mM p-nitro-phenyl-α-D-glucopyranoside (100 ml) and placed in an incubator for 15 minutes at 37 °C. The mixture's absorbance was measured at 405 nm after the addition of a 0.2 M sodium carbonate solution (400 µL) to stop the reaction. Acarbose served as a positive control in the experiment. α-glucosidase was not present in the blank solution, and DW served as a negative control. The IC_{50} values were determined by plotting concentrations against the percentage of α-glucosidase inhibition. The assay was repeated three times, with the values expressed as mean ± standard error of mean. To calculate the percentage of α-glucosidase inhibition potential, the following formula was used.

$$\%\ enzyme\ inhibition = \frac{absorbance\ of\ control - absorbance\ of\ sample}{absorbance\ of\ control} \times 100 \qquad \text{(Eq.2)}$$

Inhibition of α-amylase activity

The ability of Met-Ext-D.L and AgNPs-*D.L* to suppress the activity of α-amylase enzyme was determined through a 3,5-dinitrosalicylic acid (DNSA) test (Nazir et al., 2021). Stock solutions from both Met-Ext-D.L and AgNPs-D.L were prepared by dissolving 1 mg of each in 10% DMSO, Na_2HPO_4/NaH_2PO_4 buffer (0.02 M), and NaCl (0.006 M) at a PH of 6.9, which were then diluted in increments of 62.5 to 1000 µg/mL. Subsequently, a combination of 200 µL of the sample and a solution containing α-amylase at a concentration of 2 units/mL was prepared. This mixture was then placed in an incubator for 10 minutes at 30 °C. Each dilution was added with 200 µL of a 1% starch

http://www.aloki.hu ● ISSN 1589 1623 (Print) ● ISSN 1785 0037 (Online)
DOI: http://dx.doi.org/10.15666/aeer/2304_67876815

solution in water (w/v) following a three-minute incubation period. To stop the reaction, 200 µL of sodium potassium tartrate tetrahydrate was diluted with 20 mL of 3,5 dinitro salicylic acid and 8 mL of NaOH (2 M) (96 mM) and added to the reaction mixture. For ten minutes, the mixture was heated in a water bath between 85 and 90 °C. After cooling, 5 mL of DW was added to dilute the liquid. At 540 nm, the absorbance was determined using a UV-visible spectrophotometer. Acarbose was used as a positive control. Using the previously mentioned procedure, the reaction mixture for the positive control was produced, and absorbance was measured at 540 nm. The proportion of α-amylase inhibition against concentration was graphed to get the IC_{50} values of the sample. The assay was carried out in three replicates, and the values were expressed as the mean ± standard error of the mean. The inhibition potential of the α-amylase enzyme was calculated using the same formula as for the α-glucosidase activity (*Eq. 2*), with the appropriate variables corresponding to the α-amylase inhibition assay.

Statistical analyses

The data were analysed statistically using IBM SPSS Statistics software, version 23 (Armonk, NY, USA) and expressed as mean ± standard error of the mean (SEM). To evaluate the differences between groups, one-way analysis of variance (ANOVA) was applied, followed by Dunnett's post hoc test for pairwise comparisons. A p-value of less than 0.05 was considered to be statistically significant.

Results

GC-MS analysis of Met-Ext-D.L

Identification of different bioactive compounds in the Met-Ext of *D. longifolia* leaves was done with the help of GC-MS analysis. The compounds found in the Met-Ext-D.L were identified by comparing their mass spectra (*Table S1*: Supplementary File) with the NIST library (National Institute of Standards and Technology, 2024). The GC chromatogram (*Figure 1*) of the Met-Ext from *D. longifolia* leaves confirmed the presence of 50 compounds. The major peaks in the chromatogram corresponded to isopropyl isothiocyanate (19.15% area), Propane, 1-isothiocyanato (19.15% area), and 1,2,4-Thiadiazole, 5-amino (19.15% area), all with a retention time of 2.290 minutes. Other compounds identified in the chromatogram included Butane, 1-isothiocyanato- (1.92% area), O-Methyl N-tert-butylformimidate (1.92% area), and Glycerin (1.28% area), with retention times of 3.523 minutes and 4.020 minutes, respectively. Additionally, Diglycerol (1.28% area), Furan, 2-methyl-5-(methylthio) (1.10% area), and 2-Methoxyethyl heptanoate (1.10% area) were identified, with retention times of 4.020 minutes and 5.266 minutes, respectively.

Further compounds included 2-Amino-4,5-dimethylthiazole (1.10% area), 1,3-Dioxane-2-propanol, 2-methyl (1.02% area), and 1-cyclopropyl-3-(dimethylamino)-2-[(dimethylamino)-methyl] (1.02% area), all with retention times of 5.266 minutes and 5.791 minutes, respectively. 2-Methoxyethyl acetoacetate (1.02% area), 4,5-Diamino-2-hydroxypyrimidine (1.93% area), and D-Alanine, N-propargyloxycarbonyl-, decyl ester (1.93% area) were also present, with retention times of 5.791 minutes and 6.113 minutes, respectively. Moreover, delta.2-Tetrazaboroline, 5-ethyl-1,4-dimethyl (1.93% area), 4H-Pyran-4-one, 2,3-dihydro-3,5-dihydroxy-6-methy (1.03% area), and 2-Oxopropionic acid, dimethylhydrazone, and methyl ester (1.03% area) were detected with retention

http://www.aloki.hu ● ISSN 1589 1623 (Print) ● ISSN 1785 0037 (Online)
DOI: http://dx.doi.org/10.15666/aeer/2304_67876815

times of 6.113 minutes and 7.094 minutes, respectively. The chromatogram also revealed the presence of 5-Hydroxymethylfurfural (1.76% area), 4-Fluorobenzyl alcohol (1.76% area), and 1H-Pyrazole, 5-ethyl-4,5-dihydro-3,5-dimethy (1.76% area), all with retention times of 8.200 minutes along with many minor peaks.

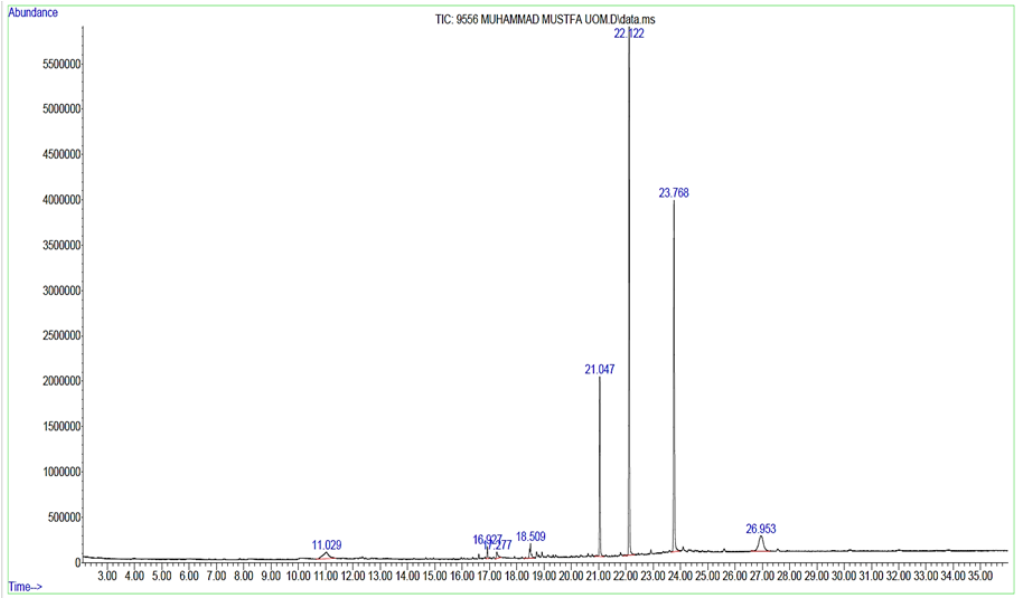

Figure 1. *GC-MS chromatogram of the Met-Ext of D. longifolia leaves*

Characterization of AgNPs of D. longifolia leaves

UV-visible spectroscopy

When the Aq-Ext-D.L was incubated with a solution of $AgNO_3$, a shift in colour occurred from colourless to dark brown, which was a confirmation of the production of AgNPs-D.L. It is well established that AgNPs in the aqueous reaction mixture are brown due to the typical surface plasmon vibrations (Mahendran et al., 2022), which can be measured using UV-visible spectroscopy. Silver ions generate a prominent peak in the range of 300-500 nm. A peak in this range confirms the synthesis of AgNPs. The different ratios of $AgNO_3$ and Met-Ext were scanned from 200 to 500 nm by a UV-Visible spectrophotometer (UV-1800 series), which showed visible peaks between 300 and 400 nm, indicating the formation of AgNPs *Figure 2(A)*. The most prominent peak was obtained in the case of 1:3, which was 322 nm *Figure 2(B)* and indicated that this ratio was optimal for synthesising more AgNPs. Hence, further synthesis was performed according to this ratio.

The bioactive substances found in the extract might have caused the reduction of silver ions into AgNPs. The extract of *D. longifolia* contains a variety of phytochemicals such as phenols, flavonols, alkaloids, flavonoids, tannins, vitamin C, vitamin E, saponins, carotenoids, chlorogenic acid, catechin, caffeic acid, coumaric acid, gallic acid, rutin, umbelliferone, ellagic acid, epicatechin, kaempferol, and total polyphenols (Kumar et al., 2015; Tapan and Kaushik, 2015; Devi, 2016; Devi et al., 2016; Radhamani and Britto, 2016).

http://www.aloki.hu ● ISSN 1589 1623 (Print) ● ISSN 1785 0037 (Online)
DOI: http://dx.doi.org/10.15666/aeer/2304_67876815

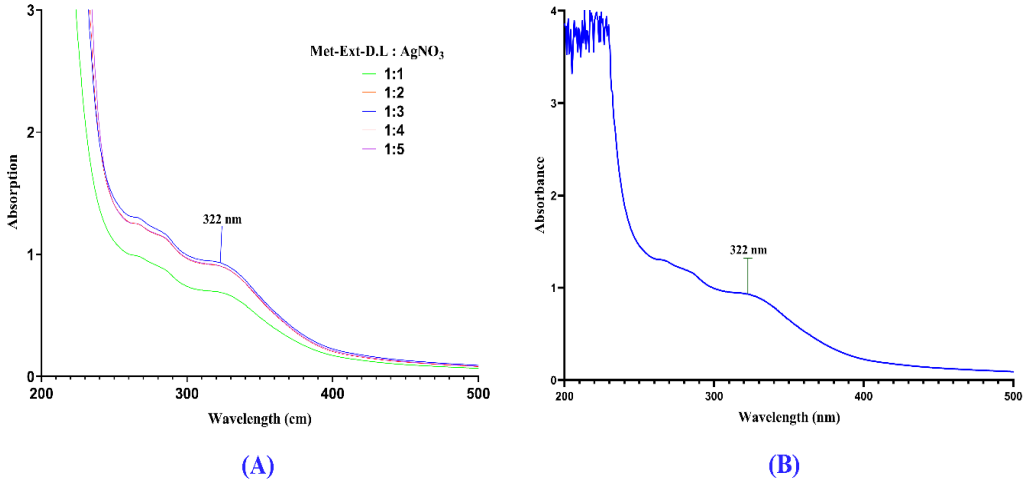

Figure 2. *(A) UV-visible spectroscopy of different ratios of Met-Ext-D.L and $AgNO_3$ from 1:1 to 1:5. (B) UV-visible spectroscopy of AgNPs synthesised from D. longifolia leaf extract*

FTIR

FTIR spectroscopy helps us identify different biomolecules present in the sample that are likely to be involved in the synthesis of AgNPs. The major visible peaks in the FTIR spectra of AgNPs-D.L are presented in *Figure 3*. Their corresponding transmittance values are reported in *Table 1*.

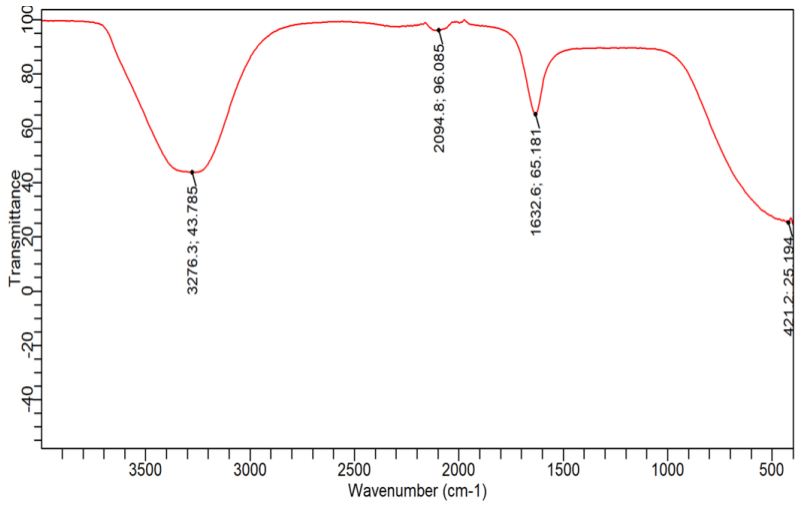

Figure 3. *FTIR spectrum of AgNPs-D.L*

Table 1. *Possible functional groups in the FTIR spectra of AgNPs-D.L*

Peak number	Wave number	Intensity	Possible functional groups
1	421.18918	25.19410	Bending vibrations in inorganic materials
2	1632.57397	65.18056	C=C stretching (alkenes), C=O stretching (conjugated systems, amides)
3	2094.76386	96.08489	C≡N stretching (nitriles), C≡C stretching (alkynes)
4	3276.32996	43.78483	O-H stretching (alcohols), N-H stretching (amines, amides)

http://www.aloki.hu ● ISSN 1589 1623 (Print) ● ISSN 1785 0037 (Online)
DOI: http://dx.doi.org/10.15666/aeer/2304_67876815

The FTIR spectrum revealed a total of 4 peaks. A broad peak was shown at 3276.33 cm^{-1} that corresponds to O-H stretching vibrations typically found in alcohols or N-H stretching vibrations associated with amines or amides (Awang et al., 2023). The second peak at 2094.76 cm^{-1} indicates the C≡N (characteristic of the nitrile group) or C≡C (characteristic of alkynes) stretching vibrations (Kikon et al., 2024). A medium-intensity peak observed at 1632.57 cm^{-1} could indicate either the presence of the C=C stretching bands, which are typical for alkenes or the C=O stretching bands, which are related to conjugated systems or amides (Huang et al., 2007; Kikon et al., 2024). A low-intensity peak observed at 421.19 cm^{-1} represents bending vibrations in inorganic materials, indicating the presence of metal-oxygen (M-O) bonds, which suggest the formation of AgNPs.

XRD

Figure 4 represents an XRD pattern shown by AgNPs-D.L. It is the most commonly used technique for analysing the crystal structure of nanomaterials. The vertical axis represents the intensity of diffracted X-rays, measured in counts per second (cps). The horizontal axis, labelled as 2θ in degrees, displays the angle at which X-rays are diffracted by the crystal planes inside the material. The graph exhibits some significant characteristics. Interestingly, separate diffraction peaks appear at particular values of 2θ. These peaks line up with the crystal structure planes that allow the diffracted X-rays to interfere constructively. The graph's overall trend indicates that intensity decreases as 2θ increases, indicating that most diffraction happens at smaller angles.

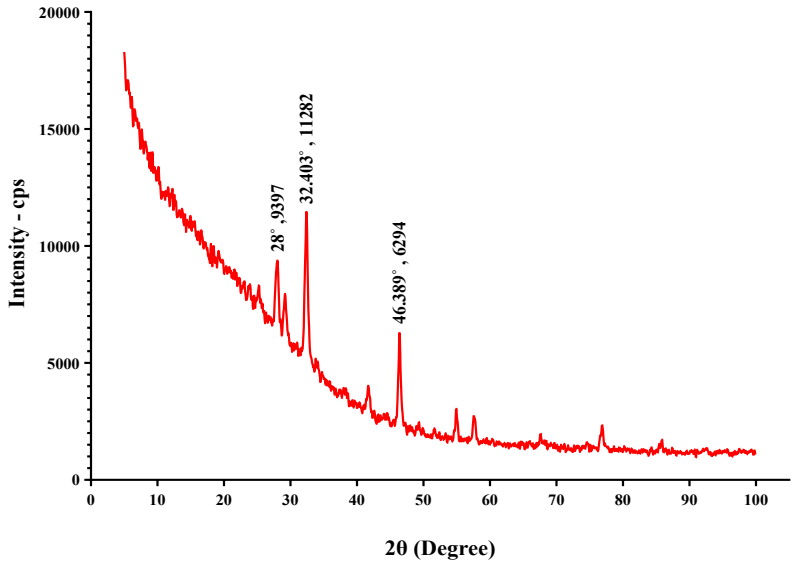

Figure 4. *X-ray diffraction analysis of AgNPs-D.L*

The most extreme peak, which is closest to 11282 cps and is located at about 32.4 degrees, can be found by carefully examining the peaks. At greater angles, there are other peaks, but they are relatively less intense. Every peak that has been seen can be linked to a particular collection of crystal planes that define AgNPs. It is possible to verify the existence of AgNPs by contrasting these peaks with accepted reference patterns for silver.

http://www.aloki.hu ● ISSN 1589 1623 (Print) ● ISSN 1785 0037 (Online)
DOI: http://dx.doi.org/10.15666/aeer/2304_67876815

The AgNPs exhibit a high degree of crystallinity, as seen by the height and sharpness of the peaks. Because nanoparticles have a significant surface area to volume ratio, wider peaks would indicate lesser crystallinity or smaller crystallite sizes. The amount of crystalline silver contained in the sample can be determined by comparing the relative strengths of the peaks. Amorphous content or smaller crystallite sizes may be present, as shown by the intensity's reduction at higher angles. The lack of peaks at extremely high angles may indicate a preferred orientation or particular crystallographic texture of the material.

EDX

EDX is used to characterise and understand the elemental composition by identifying different elements in a sample. In this study, the sample of AgNPs was analysed for the presence of silver. The predominant element detected is silver (Ag), comprising 48.77% of the sample by weight (14.12% atomic), as evident from *Figure 5*. This confirms the presence of AgNPs. The spectrum of EDX shows a strong peak for silver at 3 keV with a weightage of 48.77%, which is a characteristic of AgNPs (Balaraman et al., 2020). Besides these, there were also peaks for carbon (C), silicon (Si), oxygen (O), phosphorus (P), potassium (K), sulphur (S), calcium (Ca), and chlorine (Cl). Carbon (C) is present at 21.13% and 4.28%, respectively, indicating the presence of organic compounds or carbonates likely from the plant extract used in nanoparticle synthesis. The elements, along with their weight percentage and atomic percentage, are given in *Table 2*.

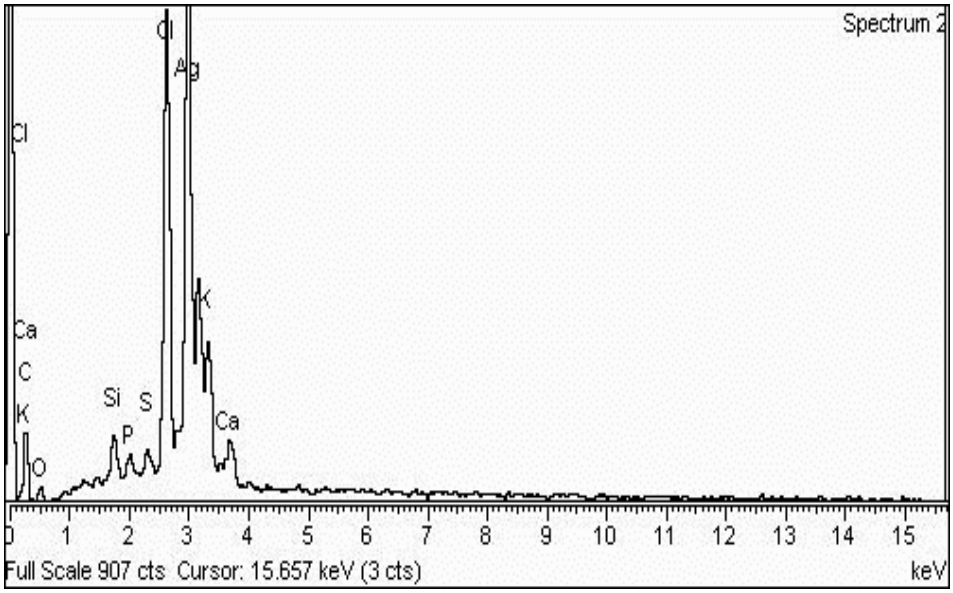

Figure 5. *EDX spectrums of AgNPs-D.L*

SEM

The distribution of AgNPs and their shape, size, and morphology were determined by SEM (Fares et al., 2024). The SEM image of the prepared AgNPs is shown in *Figure 6*. The SEM micrograph with a magnification of 10000X, reveals a heterogeneous distribution, with denser clusters in some areas. This non-uniform distribution could be due to the synthesis technique, substrate, or deposition process. The nanoparticles are

http://www.aloki.hu ● ISSN 1589 1623 (Print) ● ISSN 1785 0037 (Online)
DOI: http://dx.doi.org/10.15666/aeer/2304_67876815

mostly spherical, with sizes ranging from approximately 10 to 100 nm in diameter, although some irregularly shaped aggregates indicate slight agglomeration. The images show partial surface coverage by nanoparticles, leaving significant areas of the substrate exposed. These results confirm that the AgNPs synthesised from Aq-Ext-D.L are within the nano range.

Table 2. *Elemental composition of AgNPs-D.L determined by EDX analysis*

Element	Weight%	Atomic%
C K	21.13	54.92
O K	4.28	8.36
Si K	1.28	1.43
P K	0.74	0.75
S K	0.71	0.69
Cl K	16.48	14.51
K K	4.12	3.29
Ca K	2.48	1.93
Ag L	48.77	14.12
Total	**100.00**	

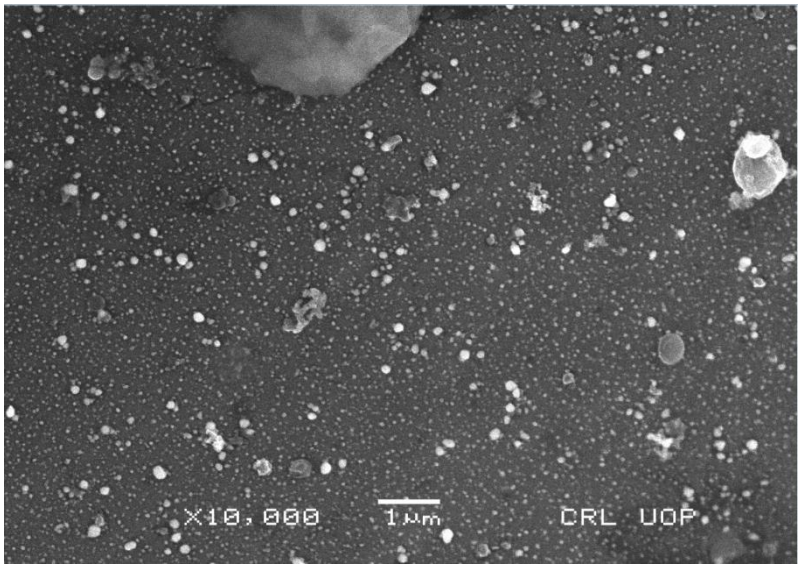

Figure 6. *SEM image of AgNPs synthesised from D. longifolia leaf extract*

Antioxidant activity

DPPH inhibition potential of AgNPs and Met-Ext of *D. longifolia* leaves are presented in *Table 3* and *Figure S1* (Supplementary File). AgNPs and Met-Ext-D.L showed %DPPH inhibition of 88±0.3*** and 77±0.9**, with their IC_{50} values 80µg/mL and 185µg/mL respectively, at the highest concentration of 1000 µg/mL. The findings showed that both AgNPs and Met-Ext of *D. longifolia* exhibit a substantial inhibitory effect, as indicated by the significant percentage of inhibition. Furthermore, the IC_{50} values of both samples are equivalent to the standard ascorbic acid, suggesting their potency. At a concentration of 1000 µg/mL, standard ascorbic acid inhibits DPPH by 94±0.1% with an IC_{50} value of 30 µg/mL.

http://www.aloki.hu ● ISSN 1589 1623 (Print) ● ISSN 1785 0037 (Online)
DOI: http://dx.doi.org/10.15666/aeer/2304_67876815

Table 3. *% DPPH free radical scavenging potential of AgNPs and Met-Ext of D. longifolia leaves*

S. No	Sample	Concentration (µg/mL)	%DPPH Scavenging	IC_{50} (µg/mL)
1	Met-Ext-D.L	1000	77±0.9**	185
		500	60±06**	
		250	54±0.5**	
		125	41±0.6**	
		62.5	39±0.5**	
2	AgNP-D.L	1000	88±0.3***	80
		500	71±0.5***	
		250	65±0.5***	
		125	59±0.4***	
		62.5	40±0.7***	
3	Ascorbic acid	1000	94±0.1	30
		500	87±0.2	
		250	75±0.1	
		125	61±0.2	
		62.5	50±0.1	

Each value is presented as mean ± SEM, with n = 3. Differences between the groups were assessed using One-Way ANOVA followed by Dunnett's post hoc test. Statistical significance was considered at $p < 0.05$, and significant differences are indicated as follows: $^{**}p < 0.01$, $^{***}p < 0.001$

Antibacterial activity

The antibacterial activity was assessed by measuring the zone around the discs that had no growth of bacteria. Both the Met-Ext-D.L and AgNPs-D.L showed inhibition of the bacterial growth, but the results of the AgNPs-D.L were better as compared to the Met-Ext-D.L. The negative control exhibited no inhibition. The Met-Ext-D.L inhibited the growth of bacteria around the discs, producing clear zones of 25 ± 0.28 mm against *P. aeruginosa*, 20 ± 0.5 mm against *K. pneumoniae*, and 25 ± 0.76 mm against *E. faecalis* (*Table 4*). Similarly, AgNPs-D.L were also effective in inhibiting bacterial growth, showing inhibition zones of 28 ± 0.5 mm for *P. aeruginosa*, 23 ± 0.28 mm for *K. pneumoniae*, and 27 ± 0.28 mm for *E.faecalis*.

Table 4. *Zone of inhibition of AgNPs-D.L, Met-Ext-D.L and standard antibiotic Imipenem against the tested bacteria*

Sample	Conc.	Zone Of Inhibition (mm)		
		PA Mean ± SEM	KP Mean ± SEM	EF Mean ± SEM
Imipenem (Standard)		30 ± 0.28	32 ± 0.5	40 ± 0.5 mm
D.W (Negative control)		-	-	-
Met-Ext-D.L	0.1mg/ml	$25 \pm 0.28^{*}$	$20 \pm 0.5^{**}$	$25 \pm 0.76^{**}$
AgNPs-D.L	0.1mg/ml	$28 \pm 0.5^{*}$	$23 \pm 0.28^{**}$	$27 \pm 0.28^{***}$

Each value is expressed as mean ± SEM, with n = 3 replicates per group. One-way ANOVA followed by Dunnett's post-hoc test was performed to evaluate differences between the groups, with statistical significance set at $^{*}p < 0.05$. Significant differences are indicated by: $^{*}p < 0.05$, $^{**}p < 0.01$, $^{***}p < 0.001$

http://www.aloki.hu ● ISSN 1589 1623 (Print) ● ISSN 1785 0037 (Online)
DOI: http://dx.doi.org/10.15666/aeer/2304_67876815

The largest zones of inhibition were observed with the standard antibiotic imipenem, with values of 30 ± 0.28 mm, 32 ± 0.5 mm, and 40 ± 0.5 mm against *P. aeruginosa*, *K. pneumoniae*, and *E. faecalis*, respectively. These results suggest that AgNPs-D.L can serve as promising antibacterial agents, especially against *P. aeruginosa*, where they exhibited stronger inhibition than Met-Ext-D.L, although the standard antibiotic still demonstrated superior performance across all strains (*Figure 7*).

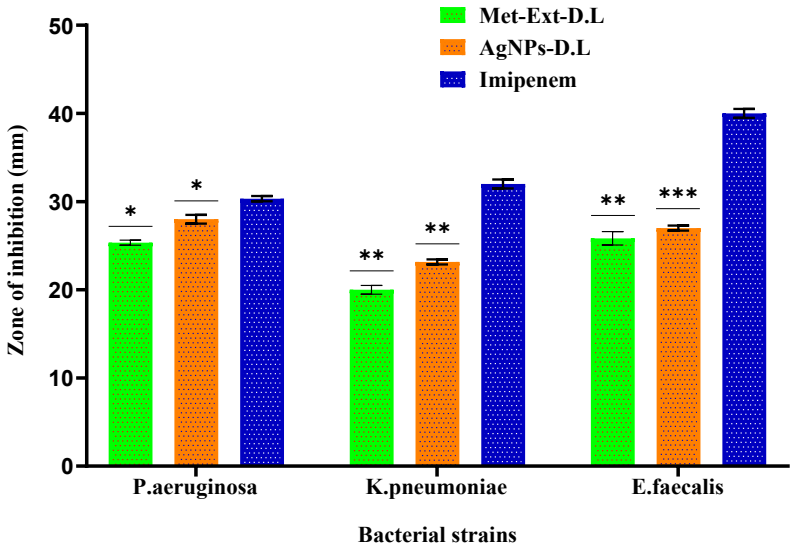

Figure 7. *% zone of inhibition of AgNPs-D.L, Met-Ext-D.L, and the standard antibiotic Imipenem against bacterial strains*

In vitro inhibition of α-amylase activity

The inhibition potential of AgNPs and Met-Ext of *D. longifolia* leaves against the α-amylase enzyme were presented in *Table 5* and *Figure S2*. The AgNPs and Met-Ext derived from *D. longifolia* leaves exhibited α-amylase inhibition of 82±0.5*** and 73±0.2*** percent respectively. The IC_{50} values for AgNPs and Met-Ext were 120µg/mL and 165µg/mL, respectively, at a maximum concentration of 1000 µg/mL. The IC_{50} values were determined by analysing the graph of % α-amylase enzyme inhibition against extract concentrations. Acarbose served as the reference compound, exhibiting a 90±0.3% inhibition rate at a maximal concentration of 1000 µg/mL, with an IC_{50} value of 30 µg/mL.

In Vitro Inhibition of α-glucosidase Activity

The IC_{50} values were calculated by plotting the percentage of α-glucosidase enzyme inhibition against the quantities of the extracts (*Table 5* and *Figure S3*). The α-glucosidase inhibition potential of AgNPs and Met-Ext of *D. longifolia* were found to be 79±0.8*** and 70±0.5** respectively, with their IC_{50} values measured at 145µg/mL and 260µg/mL, respectively, at the highest concentration of 1000 µg/mL. Acarbose served as the reference compound, exhibiting 88±0.4% inhibition at the highest concentration (1000 µg/mL), with an IC_{50} value of 40 µg/mL.

http://www.aloki.hu ● ISSN 1589 1623 (Print) ● ISSN 1785 0037 (Online)
DOI: http://dx.doi.org/10.15666/aeer/2304_67876815

Table 5. *% α-amylase and α-glucosidase inhibition potential of AgNPs and Met-Ext of D. longifolia*

S.No	Sample	Concentration (µg/mL)	% α-amylase inhibition	IC_{50} (µg/mL)	% α-glucosidase inhibition	IC_{50} (µg/mL)
			Mean ± SEM		Mean ± SEM	
1	Met-Ext-D.L	1000	73±0.2***	165	70±0.5**	260
		500	65±0.5**		62±0.6**	
		250	58±0.7**		49±0.7**	
		125	44±0.6**		40±0.5**	
		62.5	36±0.6**		35±1.5**	
2	AgNPs-D.L	1000	82±0.5***	120	79±0.8***	145
		500	74±0.9***		68±0.5***	
		250	60±0.6***		59±0.3***	
		125	50±0.5***		46±0.56***	
		62.5	43±1.6***		40±0.78***	
3	Acarbose	1000	90±0.3	30	88±0.4	40
		500	85±0.3		80±0.1	
		250	78±1.1		78±0.5	
		125	70±0.1		71±0.2	
		62.5	58±0.2		54±0.3	

Each value is expressed as mean ± SEM, with n = 3 replicates per group. One-way ANOVA followed by Dunnett's post-hoc test was performed to evaluate differences between the groups, with statistical significance set at $p < 0.05$. Significant differences are indicated by: **$p < 0.01$, ***$p < 0.001$

Discussion

For thousands of years, plants have served as the foundation of traditional medicine systems, consistently providing humanity with innovative therapeutic remedies for treating various diseases. Medicinal plants are used in more than 90% of classical medicinal formulations and cures. For about 85% of the global population, plant materials constitute a fundamental source of healthcare. Plants contain non-nutritive compounds known as phytochemicals that are well-known for having health-promoting qualities. A number of chronic medical conditions, like diabetes, bacterial infections, hypertension, cancer, heart disease, and various other diseases, are treated and/or prevented by using these phytochemicals (Ansari et al., 2025).

DM is a persistent metabolic disease marked by increased levels of glucose in the blood and compromised metabolism of carbohydrates, proteins, and lipids. The rise in glucose levels occurs due to inadequate secretion of insulin by islet cells of Langerhans in the pancreas or because of the development of resistance to insulin. In humans, DM ranks as the third most common chronic condition, following cancer and cardiovascular disease. The most prevalent type of diabetes is T2D, especially among adults aged 30 years and older, accounting for nearly 90% of the cases (Nazir et al., 2018). DM and its associated complications pose a serious threat to human health and are considered one of the top five primary contributors to global mortality. Unfortunately, the number of affected individuals is increasing rapidly. According to the International Diabetes Federation (2025) currently, 589 million individuals are diabetic, and this could increase to 853 million by the year 2045. Research findings indicate that the development of diabetes is linked to a rise in free radical production and a fall in antioxidant levels.

With the increasing prevalence of diabetes, researchers all around the world are in constant search of new antidiabetic agents that are cost-effective and efficient in treating

http://www.aloki.hu ● ISSN 1589 1623 (Print) ● ISSN 1785 0037 (Online)
DOI: http://dx.doi.org/10.15666/aeer/2304_67876815

hyperglycaemia. For this purpose, researchers consider AgNPs more useful because of their intrinsic antioxidant properties, which prove beneficial in treating oxidative stress-related disorders. Current research suggests that nanoparticles can be used in the formulation of novel antidiabetic therapies because of their ability to facilitate targeted drug delivery and their protective effects on pancreatic beta cells. As a result, nanotechnology, which uses metal nanoparticles, emerges as a versatile and promising approach to addressing the challenges posed by antibiotic resistance, oxidative stress, and diabetes.

The AgNPs formulation obtained using plant extract through the green method is the most suitable method compared to other synthesis techniques due to its multiple advantages, including enhanced surface area, solubility, and healing ability. AgNPs are suitable for targeted drug delivery systems due to their fast distribution and elimination into many body parts, such as the heart, brain, testes, liver, lungs, and kidney, as demonstrated by pharmacokinetic studies When compared to the green method, chemically produced nanoparticles displayed toxicity concerns, due to which the focus shifted towards the production of nanoparticles by the green method (Fahim et al., 2024).

In biological manufacturing, plant extract and microorganisms like fungi and bacteria are used to produce nanoparticles. Different parts of plants, like stems, roots, fruits, and leaves, are utilised to synthesise nanoparticles. Studies have shown that the presence of vitamins, proteins, organic acids, and secondary metabolites, including polysaccharides, terpenoids, flavonoids, alkaloids, and heterocyclic compounds, can induce the creation of different kinds of nanoparticles. The green method for synthesising AgNPs is highly advisable because this technique produces biocompatible, eco-friendly, cost-effective, sustainable, and scalable nanoparticles. Researchers favour using plants for nanoparticle synthesis through the green method because they are easily accessible, safe, non-toxic, and contain numerous metabolites that quickly reduce silver ions, leading to faster synthesis (Acay et al., 2019).

It has been documented in previous studies that AgNPs can be synthesised using *Debregeasia salicifolia* extracts (Khan et al., 2022). Similarly, the Met-Ext of *D. salcifolia* was used to create stable silver/gold nanoparticles (Ag/AuNPs) (Bawazeer et al., 2020). While these species have successfully generated the desired nanoparticles, other species in the *Debregeasia* genus have not yet been investigated for nanoparticle production. Therefore, in this study, we have selected another species within the genus *Debregeasia*, that is, *Debregeasia longifolia*, for synthesising AgNPs, characterising AgNPs, and assessing their biological activities. The phytochemical profile of *D. longifolia* is also investigated using GC-MS.

GC-MS was used for analysing the phytochemical profile and confirming the presence of biologically significant compounds. 50 different compounds were identified in the Met-Ext-D.L by comparing their mass spectra with those included in the NIST/NBS spectral database (*Table S1*) (National Institute of Standards and Technology, 2024). The peak area percentage represents the relative concentration of each compound in the sample. Based on this relative concentration, different compounds identified in the Met-Ext-D.L were bis (2-ethylhexyl) phthalate (31.28%), Diisooctyl phthalate (31.28%), Phthalic acid, di(2-propylpentyl) ester (31.28%), Isopropyl isothiocyanate (19.15%), Propane, 1-isothiocyanato (19.15%), 1,2,4-Thiadiazole, 5-amino (19.15%), 1H-Indol-3-ol, acetate (12.9%), 3-Morpholinone, 5-methyl-6-phenyl (12.9%), 1H-Indol-5-ol (12.9%), Benzeneacetonitrile, 4-hydroxy (7.92%), and Benzene, 1-isocyanato-4-methyl (7.92%). Besides these, many other compounds were also detected but had smaller values

http://www.aloki.hu ● ISSN 1589 1623 (Print) ● ISSN 1785 0037 (Online)
DOI: http://dx.doi.org/10.15666/aeer/2304_67876815

of peak area percentage. It has been shown that bis (2-ethylhexyl) phthalate has cytotoxic effects on the A-549 epithelial cell line and MCF-7 cell line. Additionally, it has shown antioxidant, antiviral, anticancer (El-Sayed et al., 2015), mosquito larvicidal activity, and broad-spectrum antibacterial activity (Rajamanikyam et al., 2017). Phthalic acid, di(2-propylpentyl) ester (31.28%), one of the main components in the ethanolic extract of *Onosma dichroantha's* root, has shown significant antioxidant and antibacterial activity (Pahlavan et al., 2022). Isopropyl isothiocyanate, Propane, 1-isothiocyanato, and 1,2,4-Thiadiazole, 5-amino have strong antimicrobial activity against different pathogens and contribute to the biological activity of the AgNPs-D.L (Romeo et al., 2018). The Met-Ext also contains glycerine and diglycerol, which act as capping agents and prevent agglomeration of the NPs. Previous studies have shown the presence of different phytochemical*s* in various parts of *D. longifolia* which are responsible for different pharmacological effects. Different compounds were identified in the leaves of *D. longifolia* using UHPLC. These include catechin, chlorogenic acid, coumaric acid, rutin, umbelliferone, gallic acid, ellagic acid, caffeic acid, kaempferol, epicatechin, and polyphenols (Kumar et al., 2015). All of these compounds possess strong antidiabetic activity and are responsible for the antidiabetic effect of the extract and AgNPs (Mechchate et al., 2021).

To fully characterise AgNPs and validate all their properties, a variety of techniques were employed, as a single technique is not sufficient to validate all their properties. These included UV/VIS spectrophotometry, FTIR spectroscopy, EDX spectroscopy, XRD, and SEM. Visual observation and UV spectrophotometry were used to confirm the initial formation of AgNPs from Aq-Ext-D.L and $AgNO_3$ solution. When the solutions of silver nitrate and Aq-Ext-D.L were incubated, a change in colour was observed by turning from colourless to dark brown. The UV-visible spectrophotometer serves as the primary confirmatory tool for detecting and confirming synthesised nanoparticles and to examine the reduction and stabilisation of AgNPs in aqueous solution. Silver ions in the colloidal form of nanocomposites produced a broad peak due to surface plasmon resonance (SPR), which occurs specifically when AgNPs are formed. An SPR peak produced in the range of 300–500 nm shows that AgNPs are synthesised (Seifipour et al., 2020; Khan et al., 2022). Our sample of AgNPs was examined from 200 to 800 nm by a UV visible spectrophotometer, which displayed a visible peak at 322 nm, suggesting the formation of AgNPs *Fig. 3(B)*. The increase in absorption peak intensity over time confirmed the formation of more AgNPs.

FTIR was used to identify and confirm the specific functional groups in the plant extract that help reduce silver ions to nanoparticles. FTIR analysis (*Table 1*) provides valuable insights into the molecular composition of these nanoparticles, the spectrum shows four prominent peaks: A broad peak at 3276.33 cm^{-1} corresponds to O-H stretching vibrations typically found in alcohols or N-H stretching vibrations associated with amines or amides (Awang et al., 2023). This peak shows the adsorption of water molecules on the nanoparticle surface or the presence of residual biomolecules from the leaf extract containing hydroxyl (–OH) or amine ($–NH_2$) groups. The second peak at 2094.76 cm^{-1} indicates the C≡N (characteristic of the nitrile group) or C≡C (characteristic of alkynes) stretching vibrations (Kikon et al., 2024). This distinction could be clarified by additional confirmation using complementary methods such as ^1H NMR or ^{13}C NMR spectroscopy. A medium intensity, peak observed at 1632.57 cm^{-1} could indicate either the presence of the C=C stretching bands which is typical for alkenes, or C=O stretching bands which are related to conjugated systems or amides (Huang et al., 2007). These functional groups

http://www.aloki.hu ● ISSN 1589 1623 (Print) ● ISSN 1785 0037 (Online)
DOI: http://dx.doi.org/10.15666/aeer/2304_67876815

could have arisen from biomolecules in the *D. longifolia* leaf extract used during synthesis, hence acting as capping agents in nanoparticle synthesis. A low-intensity peak observed at 421.19 cm^{-1} represents bending vibrations in inorganic materials, indicating the presence of metal-oxygen (M-O) bonds, which suggest the formation of AgNPs.

The crystalline structure of the synthesised AgNPs was characterised using XRD analysis. The XRD pattern (*Fig. 4*) showed three major peaks at $2\theta = 28^{\circ}$, 32.4° and 46.4° respectively, which corresponded to the peaks observed for elemental silver. The XRD peaks observed for the synthesised AgNPs corresponded to the (111), (200), and (220) crystallographic planes of silver. This suggests that the synthesised AgNPs exhibit a cubic crystalline structure. The findings were similar to those obtained by A. Sankaranarayanan et al. during the synthesis of nanoparticles from *Arachis hypogaea* root extract (Sankaranarayanan et al., 2017).

Further characterisation of AgNPs was performed by EDX spectroscopy, which gives information about the elemental composition of the prepared AgNPs. The spectrum showed peaks for carbon (C), silicon (Si), oxygen (O), phosphorus (P), potassium (K), sulphur (S), calcium (Ca), chlorine (Cl), and most importantly, silver (Ag). The peak for Ag was at 3 keV, showing a weight percentage of 48.77, which was a clear indication that the synthesised nanoparticles are AgNPs (Balaraman et al., 2020). The silver peak at 3 keV is similar to the peak produced by AgNPs synthesised using *Sargassum siliquosum* (Vasquez et al., 2016) and *Sargassum muticum* (Madhiyazhagan et al., 2015). The existence of carbon and oxygen is because of the organic residues from the extract. These biomolecules act as capping agents in nanoparticle synthesis and may adsorb on the surface of nanoparticles. The detection of large amounts of other elements like magnesium, silicon, and calcium suggests that these elements may originate from impurities in the reaction medium or even the plant extract.

The distribution of AgNPs and their shape, size, and morphology were determined by SEM (Fares et al., 2024). The SEM images (*Figure 6*) of the prepared AgNPs reveal a heterogeneous distribution, with denser clusters in some areas. This non-uniform distribution could be due to the synthesis technique, substrate, or deposition process. The nanoparticles are mostly spherical, with sizes ranging from approximately 10 to 100 nm in diameter, although some irregularly shaped aggregates indicate slight agglomeration. The images show partial surface coverage by nanoparticles, leaving significant areas of the substrate exposed. These results confirm that the AgNPs synthesised from Aq-Ext-D.L are within the nano range. These findings are similar to those published by Udayasoorian et al. (2011).

The Met-Ext and synthesised AgNPs were checked for different biological activities, such as antioxidant, antibacterial, and antidiabetic activities. Oxidative stress is among the major causes that lead to the development of numerous human diseases, including ageing, diabetes mellitus, cataracts, heart diseases, rheumatoid arthritis, and respiratory conditions. Free radicals are produced by metabolic processes of the cell and are characterised by the presence of unpaired valence electrons, contributing to their unstable nature, high reactivity, and independent existence. ROS and RNS make up both free radicals and other non-radical reactive species (Yoshikawa and You, 2024). Higher concentrations of both ROS and RNS can pose a risk to biomolecules due to the onset of oxidative and nitrosative stress that can result in damage to the structural integrity of various biomolecules like lipids, DNA, and proteins. Antioxidants are compounds capable of neutralising free radicals, like oxygen, nitrogen, and lipidic radicals, thereby safeguarding biological systems from their harmful effects (Ladaniya, 2023). Medicinal

http://www.aloki.hu ● ISSN 1589 1623 (Print) ● ISSN 1785 0037 (Online)
DOI: http://dx.doi.org/10.15666/aeer/2304_67876815

plants contain phytochemicals that can scavenge these free radicals and provide protection against oxidative stress and its related disorders. For evaluating the free radical scavenging potential of AgNPs and Met-Ext of *D. longifolia* leaves, the DPPH radical scavenging assay was used. DPPH is a free radical with a characteristic absorption peak at 517 nm. When antioxidants interact with DPPH, they convert it to 1,1-diphenyl-2-picryl hydrazine through rapid hydrogen acceptance. This process causes the DPPH solution to lose colour, reflecting the scavenging potential of the antioxidants in the sample. The findings of the DPPH radical scavenging assay showed that the AgNPs and Met-Ext of *D. longifolia* leaves displayed the highest potential to scavenge free radicals at a concentration of 1000 µg/ml, with percentage inhibitions of 88±0.3*** and 77±0.9** respectively with IC_{50} values of 80 µg/ml and 185 µg/ml. The results are displayed in *Table 3* and *Figure S1* (Supplementary File). However, normal ascorbic acid (1000 µg/mL), showed 94±0.1% inhibition against DPPH, with an IC_{50} value of 30 µg/ml. The IC_{50} value shows us the concentration required for scavenging half of the DPPH radicals, which in this case was found to be 80 µg/ml for AgNPs and 185 µg/ml for Met-Ext. These values indicate a substantial antioxidant potential, although they are higher than the IC_{50} value of ascorbic acid, which is 30 µg/ml. Despite the higher IC_{50} values, the significant DPPH inhibition potential of AgNPs and Met-Ext suggests that both forms of *D. longifolia* possess strong antioxidant properties, which can be attributed to its rich phytochemical profile that possesses different compounds with strong antioxidant activity like bis (2-ethylhexyl) (El-Sayed et al., 2015), phthalic acid, di(2-propylpentyl) ester (Pahlavan, Babanejad and Band, 2022), catechin, kaempferol, gallic acid, coumaric acid, chlorogenic acid, epicatechin, caffeic acid, and other compounds (Mechchate et al., 2021).

With the alarming rise of antibiotic resistance, researchers all over the world are in constant search of innovative antimicrobial agents that are cost-effective and capable of combating resistance issues. This growing need has led researchers to use nanotechnology, specifically metal nanoparticles, to find alternatives to conventional antibiotics. Research has shown that metal nanoparticles synthesised from plants using green methods are essential for drug delivery systems and possess effective antimicrobial activity, making them useful against various microbes (Mittal et al., 2017). Due to their enhanced permeability through microbial cell walls and membranes, metal nanoparticles exhibit broad-spectrum antiseptic activity and superior efficacy compared to conventional antibiotics. This improved penetration disrupts vital cellular processes, resulting in diverse bactericidal mechanisms and a reduced likelihood of resistance development. Additionally, certain nanoparticles exhibit inherent antioxidant properties, providing potential benefits in combating oxidative stress-related disorders.

In this study, the antibacterial activity of AgNPs and Met-Ext of *D. longifolia* leaves was assessed using the Kirby-Bauer disc diffusion method, following the guidelines of CLSI (2012). The antibacterial activity was assessed against Gram-positive bacteria, including *E. faecalis*, and Gram-negative bacteria, including *K. pneumoniae* and *P. aeruginosa*. Antibiotic discs of imipenem were used as a standard. Both the Met-Ext-D.L and AgNPs-D.L were efficient at inhibiting the development of bacteria, but the results of the AgNPs-D.L were better as compared to the Met-Ext-D.L, as shown in *Table 4*. The Met-Ext-D.L demonstrated promising antibacterial activity, with inhibition zones of 25 ± 0.28 mm against *P. aeruginosa*, 20 ± 0.5 mm against *K. pneumoniae*, and 25 ± 0.76 mm against *E. faecalis*. However, when AgNPs-D.L were tested, the inhibition zones were larger, measuring 28 ± 0.5 mm against *P. aeruginosa*, 23 ± 0.28 mm against

http://www.aloki.hu ● ISSN 1589 1623 (Print) ● ISSN 1785 0037 (Online)
DOI: http://dx.doi.org/10.15666/aeer/2304_67876815

K. pneumoniae, and 27 ± 0.28 mm against *E. faecalis*. The negative control showed no inhibition, confirming that the observed antibacterial effects were due to the agents being tested. These results indicate that both Met-Ext-D.L and AgNPs-D.L were effective in inhibiting bacterial growth, particularly against *P. aeruginosa* and *E. faecalis* (*Figure 7*), which are known to be resistant to many antibiotics. However, it is important to note that the standard antibiotic imipenem showed the largest zones of inhibition across all bacterial strains, with inhibition zones of 30 ± 0.28 mm against *P. aeruginosa*, 32±0.5 mm against *K. pneumoniae*, and 40 ± 0.5 mm against *E. faecalis*. While AgNPs-D.L showed promising antibacterial activity, imipenem, as a standard antibiotic, still demonstrated superior performance overall. The antibacterial property of AgNPs is due to their ability to release Ag^+ ions that can easily penetrate bacterial cells and bind to the cellular components, causing damage to the cell membranes. This increases cell permeability, which interrupts energy production and causes bacterial cell death. Electrostatic forces play an important role in the interaction between silver ions and bacteria by attracting positively charged Ag^+ ions to negatively charged bacterial surfaces. Silver ions can also cause cell death by inhibiting DNA replication and cell division by binding to thiol groups in bacterial enzymes and DNA (Nurkhaliza et al., 2024).

Met-Ext-D.L and AgNPs-D.L were evaluated for their antidiabetic potential utilising in vitro experiments targeting key enzymes involved in glucose metabolism (α-amylase and α-glucosidase). The inhibition of α-amylase and α-glucosidase in anti-diabetic assays is a well-established approach to prevent postprandial hyperglycaemia. The α-amylase enzyme plays an important role in the breakdown of starch into disaccharides, which are then hydrolysed by the enzyme α-glucosidase into simple sugars. These simple sugars can be easily absorbed by the small intestine, leading to an increased level of blood glucose after meals. Therefore, by blocking these enzymes, starch digestion is slowed, which reduces the absorption of glucose and helps lower blood sugar levels after meals (Nazir et al., 2018). In our study both, the AgNPs and Met-Ext successfully inhibited α-amylase and α-glucosidase in a dose-dependent manner. AgNPs proved to be more potent inhibitors of these enzymes compared to the Met-Ext. The inhibitory activity of both AgNPs and Met-Ext against the α-amylase enzyme is presented in *Table 5* and *Figure S2* and against α-glucosidase in *Table 5* and *Figure S3*. The AgNPs exhibited a strong inhibitory effect with an inhibition percentage of 82±0.5% at the highest concentration of 1000 µg/mL and an IC_{50} value of 120 µg/mL against α-amylase and an inhibition percentage of 79±0.8% and an IC_{50} value of 145 µg/mL at the highest concentration of 1000 µg/mL against α-glucosidase. In comparison, the Met-Ext displayed a slightly lower inhibition percentage of 73±0.2% at the same concentration, with an IC_{50} value of 165 µg/mL against α-amylase and 70±0.5% inhibition with an IC_{50} value of 260 µg/mL at the same concentration against α-glucosidase. A standard antidiabetic drug, acarbose, was utilised, which demonstrated 90±0.3% inhibition of the amylase enzyme with an IC_{50} value of 30 µg/mL against α-amylase and 88±0.4% inhibition with an IC_{50} value of 40 µg/mL against α-glucosidase.

The results showed that AgNPs had a greater inhibitory impact compared to the Met-Ext of *D. longifolia* in the α-amylase and α-glucosidase inhibitory assays. It is mainly due to the nano size of AgNPs that gives them a greater surface area, which boosts their capacity to enter and interact with enzymes more efficiently. AgNPs also have the ability to target and attach to particular enzyme areas that are inaccessible to bigger particles or molecules, hence enhancing their effectiveness in inhibiting enzymes.

http://www.aloki.hu ● ISSN 1589 1623 (Print) ● ISSN 1785 0037 (Online)
DOI: http://dx.doi.org/10.15666/aeer/2304_67876815

Conclusion

In this research, AgNPs were successfully synthesised through a cost-efficient, easy, precise, and environmentally sustainable green method from the aqueous extract of *D. longifolia leaves*. *D. longifolia* contains numerous phytochemicals, including phenols, flavonoids, flavonols, alkaloids, tannins, saponins, vitamin C, vitamin E, and carotenoids, which act as both reducing agents for reducing Ag^+ into Ag^0 and as capping agents for stabilising AgNPs. The synthesis of AgNPs was confirmed initially by a change of colour from colourless to brown and with different characterisation techniques like UV-visible spectroscopy, FTIR spectroscopy, XRD, EDX, and SEM. The specific SPR peak was shown by the UV-visible spectroscopy, confirming the synthesis of AgNPs. The FTIR revealed the presence of functional groups on the surface of AgNPs, which assisted in its synthesis. XRD confirmed that the crystalline structure of the synthesised AgNPs is cubic in nature. The EDX revealed silver as a major element in the composition of AgNPs, and SEM analysis revealed that AgNPs are spherical with a size of 10-100 nm. The DPPH assay showed that both AgNPs and Met-Ext-D.L were effective in scavenging free radicals and showed comparable results to the standard ascorbic acid. The antibacterial assay showed that both the Met-Ext-D.L and AgNPs-D.L were capable of inhibiting bacterial growth, but the results of the AgNPs-D.L were better as compared to the Met-Ext-D.L and even better than the antibiotic in the case of the strain *P. aeruginosa*. Similarly, AgNPs-D.L and Met-Ext-D.L were also effective in inhibiting the activity of α-amylase and α-glucosidase in a dose-dependent manner. They showed comparable results to the standard acarbose. These results showed that AgNPs-D.L have the potential to be an important component in many biomedical applications, including the treatment of severe ailments like diabetes and cancer. Additionally, they may be used as an antibacterial agent in wound dressings.

Conflict of interest. The authors declare no conflict of interest.

Authors' contributions. Conceptualization, Nausheen Nazir; methodology, Muhammad Mustafa and Jawad Hussain; software, Atiya Azam; validation, Jahangir Khan and Fahad Al-Asmari and Maher S Alwethaynani; formal analysis, Mohammad Nisar.; investigation, Fakhria Al Joufi, resources, Tariq Aziz.; data curation, Aziza Mahdy Nahari.; writing—original draft preparation, Jawad Hussain.; writing—review and editing, Shaza Abdullah Alyamani; visualization, Fahad Al Asmari; supervision, Nausheen Nazir and Tariq Aziz.; project administration, Tariq Aziz.

Acknowledgement. The authors are thankful to the Deanship of Scientific Research (DSR) at King Faisal University under project no. [KFU252733].

REFERENCES

[1] Acay, H., Baran, M. F., Eren, A. (2019): Investigating antimicrobial activity of silver nanoparticles produced through green synthesis using leaf extract of common grape (*Vitis vinifera*). – Applied Ecology & Environmental Research 17(2): 4539-4546. https://doi.org/10.15666/aeer/1702_45394546.

[2] Altammar, K. A. (2023): A review on nanoparticles: characteristics, synthesis, applications, and challenges. – Frontiers in Microbiology 14: 1155622. https://doi.org/10.3389/fmicb.2023.1155622.

[3] Ansari, P., Reberio, A. D., Ansari, N. J., Kumar, S., Khan, J. T., Chowdhury, S., Abd El-Mordy, F. M., Hannan, J. M. A., Flatt, P. R., Abdel-Wahab, Y. H. A., Seidel, V. (2025):

http://www.aloki.hu ● ISSN 1589 1623 (Print) ● ISSN 1785 0037 (Online)
DOI: http://dx.doi.org/10.15666/aeer/2304_67876815

Therapeutic Potential of Medicinal Plants and Their Phytoconstituents in Diabetes, Cancer, Infections, Cardiovascular Diseases, Inflammation and Gastrointestinal Disorders. – Biomedicines 13(2): 454. https://doi.org/10.3390/biomedicines13020454.

[4] Awang, N. A., Zulkefli, N. U. H. H., Zamri, A. Z. M., Bt N Mahmud, N. N. H. E., Muhammad, N. A. M. (2023): Enhanced tunability of Q-switched fiber lasers using biogenic AgNPs-Cs saturable absorber: optical deposition vs. drop casting. – NAM. https://doi.org/10.2139/ssrn.4585228.

[5] Balaraman, P., Balasubramanian, B., Kaliannan, D., Durai, M., Kamyab, H., Park, S., Chelliapan, S., Lee, C. T., Maluventhen, V., Maruthupandian, A. (2020): Phyco-synthesis of silver nanoparticles mediated from marine algae *Sargassum myriocystum* and its potential biological and environmental applications. – Waste and Biomass Valorization 11: 5255-5271. https://link.springer.com/article/10.1007/s12649-020-01083-5.

[6] Bawazeer, S., Rauf, A., Rahman, K. U., Ali, J., Uddin, G., Begum, F., Mubarak, M. S., Ramadan, M. F. (2020): Green synthesis and antimicrobial potential of silver/gold nanoparticles functionalized with Debregeasia Salicifolia D. Don. – Journal of Pure and Applied Microbiology 14: 2513-2523. https://doi.org/10.22207/JPAM.14.4.28.

[7] Bhardwaj, B., Singh, P., Kumar, A., Kumar, S., Budhwar, V. (2020): Eco-friendly greener synthesis of nanoparticles. – Advanced Pharmaceutical Bulletin 10(4): 566-576. https://doi.org/10.34172/apb.2020.067.

[8] Brand-Williams, W., Cuvelier, M.-E., Berset, C. (1995): Use of a free radical method to evaluate antioxidant activity. – LWT-Food Science and Technology 28(1): 25-30. https://doi.org/10.1016/S0023-6438(95)80008-5.

[9] CLSI (2012): Performance Standards for Antimicrobial Disk Susceptibility Tests; Approved Standard. – 11th ed. Vol. 32, Clinical and Laboratory Standards Institute.

[10] Devi, O. A., Chongtham, C. (2016): In-vitro antioxidant profile and reducing power of five medicinal plants of Manipur having anti-inflammatory properties. – International Journal of Current Research 8(5): 31402-31408.

[11] Devi, O. A., Das, M., Saikia, A., Das, P. (2016): Ascorbic acid and tocopherol content of ten medicinal plant extracts of Manipur having anti-inflammatory properties. – International Journal of Home Science 2(1): 308-312.

[12] Dhale, D. A., Sharma, J. (eds.) (2023): Recent Developments in Nanoscience and Nanotechnology: An Overview. – Book Rivers, India.

[13] Dhand, C., Dwivedi, N., Loh, X. J., Ying, A. N. J., Verma, N. K., Beuerman, R. W., Lakshminarayanan, R., Ramakrishna, S. (2015): Methods and strategies for the synthesis of diverse nanoparticles and their applications: a comprehensive overview. – RSC Advances 5(127): 105003-105037. https://doi.org/10.1039/C5RA19388E.

[14] El-Sayed, O. H., Asker, M. M. S., Shash, S. M., Hamed, S. R. (2015): Isolation, structure elucidation, and biological activity of di-(2-ethylhexyl) phthalate produced by Penicillium janthinellum 62. – International Journal of Chemical Technology Research 8(1): 58-66.

[15] Fahim, M., Shahzaib, A., Nishat, N., Jahan, A., Bhat, T. A., Inam, A. (2024): Green synthesis of silver nanoparticles: A comprehensive review of methods, influencing factors, and applications. – JCIS Open 16: 100125. https://doi.org/10.1016/j.jciso.2024.100125.

[16] Fares, A., Mahdy, A., Ahmed, G. (2024): Unraveling the mysteries of silver nanoparticles: Synthesis, characterization, antimicrobial effects, and uptake translocation in plants—a review. – Planta 260(1): 7. https://doi.org/10.1007/s00425-024-04439-6.

[17] Huang, J., Li, Q., Sun, D., Lu, Y., Su, Y., Yang, X., Wang, H., Wang, Y., Shao, W., He, N. (2007): Biosynthesis of silver and gold nanoparticles by novel sundried *Cinnamomum camphora* leaf. – Nanotechnology 18(10): 105104. https://doi.org/10.1088/0957-4484/18/10/105104.

[18] Hussain, I., Singh, N. B., Singh, A., Singh, H., Singh, S. C. (2016): Green synthesis of nanoparticles and its potential application. – Biotechnology Letters 38: 545-560. https://doi.org/10.1007/s10529-015-2026-7.

http://www.aloki.hu ● ISSN 1589 1623 (Print) ● ISSN 1785 0037 (Online)
DOI: http://dx.doi.org/10.15666/aeer/2304_67876815

[19] India Biodiversity Portal (n.d.): Debregeasia longifolia (Burm. F.) Wedd. | Species. – https://indiabiodiversity.org/species/show/10016. Accessed 29 May.
[20] International Diabetes Federation (2025): IDF Diabetes Atlas. – Available at: https://www.diabetesatlas.org.
[21] Khan, J., Naseem, I., Bibi, S., Ahmad, S., Altaf, F., Hafeez, M., Almoneef, M. M., Ahmad, K. (2022): Green synthesis of silver nanoparticles (Ag-NPs) using *Debregeasia salicifolia* for biological applications. – Materials 16(1): 129. https://doi.org/10.3390/ma16010129.
[22] Kikon, L., Sumedha, N., Rajaganesh, K., Chamuah, J., Rupreo, V., Baranitharan, M., Gokulakrishnan, J. (2024): Green synthesis of silver nanoparticles from *Parkia speciosa* seeds and pods extract: characterization and antioxidant properties for biomedical and nanotechnological applications. – Biochemical & Cellular Archives 24(1): 405. http://dx.doi.org/10.51470/bca.2024.24.1.405.
[23] Kumar, V., Sharma, A., Bhardwaj, R., Thukral, A. (2015): Polyphenol profiling in the leaves of plants from the catchment area of river Beas, India. – International Journal of Pharma and Bio Sciences 6: B1005-B1012.
[24] Ladaniya, M. (2023): Fruit biochemistry. – In: Ladaniya, M. (ed.) Citrus Fruit (Second Edition). Chapter 6, Academic Press, pp. 173-247. https://doi.org/10.1016/B978-0-323-99306-7.00021-9.
[25] Madhiyazhagan, P., Murugan, K., Kumar, A. N., Nataraj, T., Dinesh, D., Panneerselvam, C., Subramaniam, J., Kumar, P. M., Suresh, U., Roni, M. (2015): *Sargassum muticum*-synthesized silver nanoparticles: an effective control tool against mosquito vectors and bacterial pathogens. – Parasitology Research 114: 4305-4317. https://doi.org/10.1007/s00436-015-4671-0.
[26] Mahendran, N., Anand, B., Rajarajan, M., Muthuvel, A., Mohana, V. (2022): Green Synthesis, Characterization, and Antimicrobial Activities of Silver Nanoparticles Using Cissus Quadarangularis Leaf Extract. – Materials Today: Proceedings 49: 2620-2623. https://doi.org/10.1016/j.matpr.2021.08.043.
[27] Mahmoud, N. M. O. (2019): Debregeasia Longifolia: Biochemistry, Functions and Utilization. – In: Wild Fruits: Composition, Nutritional Value, and Products, pp. 371-377.
[28] Mariani, R., Sukandar, E. Y., Suganda, A. G. (2014): Antimicrobial activity from Indonesian Urticaceae. – International Journal of Pharmacy and Pharmaceutical Sciences 6(4): 191-193.
[29] Mechchate, H., Es-Safi, I., Haddad, H., Bekkari, H., Grafov, A., Bousta, D. (2021): Combination of Catechin, Epicatechin, and Rutin: Optimization of a Novel Complete Antidiabetic Formulation Using a Mixture Design Approach. – The Journal of Nutritional Biochemistry 88: 108520. https://doi.org/10.1016/j.jnutbio.2020.108520.
[30] Mittal, J., Singh, A., Batra, A., Sharma, M. M. (2017): Synthesis and Characterization of Silver Nanoparticles and Their Antimicrobial Efficacy. – Particulate Science and Technology 35(3): 338-345. https://doi.org/10.1080/02726351.2016.1158757.
[31] Nadaroglu, H., Güngör, A. A., Ince, S. (2017): Synthesis of Nanoparticles by Green Synthesis Method. – International Journal of Innovative Research and Reviews 1(1): 6-9.
[32] National Institute of Standards and Technology (2024): NIST Inorganic Crystal Structure Database. – National Institute of Standards and Technology, Gaithersburg, MD 20899. Accessed 10 August. https://doi.org/10.18434/M32147.
[33] Nazir, N., Zahoor, M., Nisar, M., Khan, I., Karim, N., Abdel-Halim, H., Ali, A. (2018): Phytochemical analysis and antidiabetic potential of *Elaeagnus umbellata* (Thunb.) in streptozotocin-induced diabetic rats: Pharmacological and computational approach. – BMC Complementary and Alternative Medicine 18. https://doi.org/10.1186/s12906-018-2381-8.
[34] Nazir, N., Zahoor, M., Uddin, F., Nisar, M. (2021): Chemical Composition, in Vitro Antioxidant, Anticholinesterase, and Antidiabetic Potential of Essential Oil of *Elaeagnus umbellata* Thunb. – BMC Complementary Medicine and Therapies 21: 1-13. https://doi.org/10.1186/s12906-021-03228-y.

http://www.aloki.hu ● ISSN 1589 1623 (Print) ● ISSN 1785 0037 (Online)
DOI: http://dx.doi.org/10.15666/aeer/2304_67876815

[35] Nurkhaliza, F., Risana, M. Z., Pubasari, A., Priatmoko, S., Prastya, M. E., Andreani, A. S. (2024): Comparative study of well diffusion and disc diffusion method to investigate the antibacterial properties of silver nanoparticles synthesized from *Curcuma longa* extracts. – E3S Web of Conferences 09003. EDP Sciences.

[36] Pahlavan, P., Babanejad, H., Band, S. S. (2022): Phytochemical composition, antibacterial and antioxidant activities of the ethanolic root extract of the endemic Onosma, northern Iran. – Research Square, preprint. https://doi.org/http://dx.doi.org/10.21203/rs.3.rs-1353931/v1.

[37] Patil, R. B., Chougale, A. D. (2021): Analytical methods for the identification and characterization of silver nanoparticles: A brief review. – Materials Today: Proceedings, 47: 5520-5532. https://doi.org/10.1016/j.matpr.2021.03.384.

[38] Plants of the World Online | Kew Science (accessed 29 May): *Debregeasia longifolia* (Burm. f.) Wedd. – Royal Botanic Gardens, Kew. https://powo.science.kew.org/taxon/851412-1#higher-classification.

[39] Radhamani, T., Britto, J. S. (2016): Screening of preliminary phytochemicals and their free radical scavenging activities of ethanolic extracts of *Toddalia asiatica* (L.) Lam., *Debregeasia longifolia* (Burm. f.) Wedd., and *Polygala arillata* Buch.-Ham ex Don. – International Journal of Engineering Research and Applications 6(1): 151-160.

[40] Rai, M., Yadav, A., Gade, A. (2009): Silver nanoparticles as a new generation of antimicrobials. – Biotechnology Advances 27(1): 76-83. https://doi.org/10.1016/j.biotechadv.2008.09.002.

[41] Rajamanikyam, M., Vadlapudi, V., Parvathaneni, S. P., Koude, D., Sripadi, P., Misra, S., Amanchy, R., Upadhyayula, S. M. (2017): Isolation and characterization of phthalates from Brevibacterium mcbrellneri that cause cytotoxicity and cell cycle arrest. – EXCLI Journal 16: 375. https://doi.org/10.17179/excli2017-145.

[42] Ramya, M., Subapriya, M. S. (2012): Green synthesis of silver nanoparticles. – International Journal of Pharmaceutics, Medical and Biological Sciences 1(1): 54-61.

[43] Romeo, L., Iori, R., Rollin, P., Bramanti, P., Mazzon, E. (2018): Isothiocyanates: An overview of their antimicrobial activity against human infections. – Molecules 23(3): 624. https://doi.org/10.3390/molecules23030624.

[44] Sankaranarayanan, A., Munivel, G., Karunakaran, G., Kadaikunnan, S., Alharbi, N. S., Khaled, J. M., Kuznetsov, D. (2017): Green synthesis of silver nanoparticles using *Arachis hypogaea* (ground nut) root extract for antibacterial and clinical applications. – Journal of Cluster Science 28: 995-1008. https://doi.org/10.1007/s10876-016-1084-x.

[45] Seifipour, R., Nozari, M., Pishkar, L. (2020): Green synthesis of silver nanoparticles using *Tragopogon collinus* leaf extract and study of their antibacterial effects. – Journal of Inorganic and Organometallic Polymers and Materials 30(8): 2926-2936. https://doi.org/10.1007/s10904-020-01441-9.

[46] Tapan, S., Kaushik, C. (2015): Antioxidant activities of five wild edible fruits of Meghalaya state in India and effect of solvent extraction system. – International Journal of Pharmaceutical Sciences and Research (IJPSR) 6: 5134-5140.

[47] The World Flora Online (2024): "Urticaceae Juss.". – Accessed 28 May from: https://www.worldfloraonline.org/taxon/wfo-7000000631;jsessionid=647B800368AB14AA4D1F510BC95CAC9D#local.

[48] Udayasoorian, C., Kumar, K. V., Jayabalakrishnan, M. (2011): Extracellular synthesis of silver nanoparticles using leaf extract of *Cassia auriculata*. – Digest Journal of Nanomaterials and Biostructures 6: 279-283.

[49] Vasquez, R. D., Apostol, J. G., de Leon, J. D., Mariano, J. D., Mirhan, C. M. C., Pangan, S. S., Reyes, A. G. M., Zamora, E. T. (2016): Polysaccharide-mediated green synthesis of silver nanoparticles from *Sargassum siliquosum* JG Agardh: Assessment of toxicity and hepatoprotective activity. – OpenNano 1: 16-24. https://doi.org/10.1016/j.onano.2016.03.001.

http://www.aloki.hu ● ISSN 1589 1623 (Print) ● ISSN 1785 0037 (Online)
DOI: http://dx.doi.org/10.15666/aeer/2304_67876815

[50] World Flora Online (2024): Debregeasia Gaudich. – Available at: https://www.worldfloraonline.org/taxon/wfo-4000010901 (Accessed: 29 May).
[51] Yang, S. (2021): Characterization of Silver Nanoparticles. – In: Lal, H. M., Thomas, S., Li, T., Maria, H. J. (eds.) Polymer Nanocomposites Based on Silver Nanoparticles. Engineering Materials. Springer, Cham. https://doi.org/10.1007/978-3-030-44259-0_4.
[52] Yoshikawa, T., You, F. (2024): Oxidative stress and bio-regulation. – International Journal of Molecular Sciences 25: 63360. https://doi.org/10.3390/ijms25063360.

APPENDIX

Table S1. *Parameters of various phytochemicals identified in Met-Ext of D. longifolia leaves*

No.	Compound	MF	MW	RT (min)	Peak area	% Area
1	Isopropyl isothiocyanate	C_4H_7NS	101.167	2.290	5736046	19.15
2	Propane, 1-isothiocyanato	C_4H_7NS	101.170	2.290	5736046	19.15
3	1,2,4-Thiadiazole, 5-amino	$C_2H_3N_3S$	101.130	2.290	5736046	19.15
4	Butane, 1-isothiocyanato-	C_5H_9NS	115.197	3.523	574729	1.92
5	O-Methyl N-tert-butylformimidate		166.17	3.523	574729	1.92
6	Glycerin	$C_3H_8O_3$	92.093	4.020	384229	1.28
7	Diglycerol	$C_6H_{14}O_5$	166.17	4.020	384229	1.28
8	Furan, 2-methyl-5-(methylthio)	C_6H_8OS	128.192	5.266	328911	1.10
9	2-Methoxyethyl heptanoate	$C_{10}H_{20}O_3$	188.264	5.266	328911	1.10
10	2-Amino-4,5-dimethylthiazole	$C_5H_8N_2S$	128.199	5.266	328911	1.10
11	1,3-Dioxane-2-propanol, 2-methyl	$C_8H_{16}O_3$	160.21	5.791	305956	1.02
12	1-cyclopropyl-3-(dimethylamino)-2-[(dimethylamino)methyl]	$C_{11}H_{21}N_3$	195.3	5.791	305956	1.02
13	2-Methoxyethyl acetoacetate	$C_7H_{12}O_4$	160.17	5.791	305956	1.02
14	4,5-Diamino-2-hydroxypyrimidine	$C_4H_5N_3O$	113.11	6.113	578168	1.93
15	D-Alanine, N-propargyloxycarbonyl-, decyl ester	$C_{17}H_{29}NO_4$	311.4	6.113	578168	1.93
16	.delta.2-Tetrazaboroline, 5-ethyl-1,4-dimethyl	$C_4H_{11}BN_4$	126.0	6.113	578168	1.93
17	4H-Pyran-4-one, 2,3-dihydro-3,5-dihydroxy-6-methyl	$C_6H_8O_4$	144.12	7.094	308454	1.03
18	2-Oxopropionic acid, dimethylhydrazone, methyl ester	$C_6H_{12}N_2O_2$	144.17	7.094	308454	1.03
19	5-Hydroxymethylfurfural	$C_6H_6O_3$	126.11	8.200	527118	1.76
20	4-Fluorobenzyl alcohol	C_7H_7FO	126.13	8.200	527118	1.76
21	1H-Pyrazole, 5-ethyl-4,5-dihydro-3,5-dimethy	$C_8H_{14}N_2$	138.2	8.200	527118	1.76
22	1,3-Dioxolane, 2-ethenyl-4-methyl-	$C_6H_8O_2$	112.13	9.229	340989	1.14
23	Hydrazine, 1,1-diethyl-2-(1-methylpropyl)	$C_6H_{16}N_2$	116.205	9.229	340989	1.14
24	Oxazolidin-2-one	$C_3H_5NO_2$	87.078	9.229	340989	1.14
25	Tetrahydro-1,3-oxazine-2-thione	C_4H_7NOS	117.169	10.812	364551	1.22
26	2-Thio-2,4-oxazolidinedione	$C_3H_3NO_2S$	117.13	10.812	364551	1.22
27	Dimethyl 3,6,9,12,15,18,21-heptaoxatricosane-1,23-dioate	$C_{25}H_{42}O_{10}$	502.6	10.812	364551	1.22
28	1,3-Dioxane-5-methanol, 5-ethyl	$C_7H_{14}O_3$	146.18	11.330	798290	2.67
29	1-Butanol, 4-butoxy	$C_8H_{18}O_2$	146.23	11.330	798290	2.67
30	1,4,2,5 Cyclohexanetetrol	$C_6H_4O_4$	140.09	11.330	798290	2.67
31	Benzeneacetonitrile, 4-hydroxy	C_8H_7NO	133.15	11.722	2370516	7.92

http://www.aloki.hu ● ISSN 1589 1623 (Print) ● ISSN 1785 0037 (Online)
DOI: http://dx.doi.org/10.15666/aeer/2304_67876815

No.	Compound	MF	MW	RT (min)	Peak area	% Area
32	Benzene, 1-isocyanato-4-methy	C_8H_7NO	133.15	11.722	2370516	7.92
33	d-Gala-l-ido-octonic amide	$C_8H_{17}NO_8$	255.22	13.010	972013	3.25
34	.beta.-D-Glucopyranose, 4-O-.beta.-D-galactopyranosyl	$C_{12}H_{22}O_{11}$	342.3	13.010	972013	3.25
35	d-Manno-l-gluco-octonic acid	$C_8H_{16}O_9$	256.21	13.010	972013	3.25
36	4-Nitro-2-pyridinecarbonitrile	$C_6H_3N_3O_2$	149.11	14.733	822717	2.75
37	6-Methylthieno[2,3-b]pyridine	C_8H_7NS	149.21	14.733	822717	2.75
38	1H-Purin-6-amine, N-methyl-	$C_6H_7N_5$	149.153	14.733	822717	2.75
39	n-Hexadecanoic acid	$C_{16}H_{32}O_2$	256.424	17.373	537375	1.79
40	1,3,5-Triazin-2(1H)-one, 5,6-dihydro-5,5-bis(trifluoromethyl)-4-phenyl	$C_{12}H_8F_6N_3O^+$	324.2	18.955	333472	1.11
41	Benzo[1,2-b:5,4-b']difuran-4,8-dione, 5-methyl-2-(1-methylethenyl) 2	$C_{14}H_{10}O_4$	242.23	18.955	333472	1.11
42	Benzo[c]phenanthrene, 5-methyl-	$C_{19}H_{14}$	242.314	18.955	333472	1.11
43	Octadecanoic acid	$C_{18}H_{36}O_2$	284.477	19.228	411965	1.38
44	1H-Indol-3-ol, acetate	$C_{10}H_9NO_2$	175.18	21.357	3863659	12.9
45	3-Morpholinone, 5-methyl-6-phenyl	$C_{11}H_{13}NO_2$	191.226	21.357	3863659	12.9
46	1H-Indol-5-ol	C_8H_7NO	133.147	21.357	3863659	12.9
47	Bis(2-ethylhexyl) phthalateDiisooctyl phthalate	$C_{24}H_{38}O_4$	390.6	22.239	9366144	31.28
48	Diisooctyl phthalate	$C_{24}H_{38}O_4$	390.6	22.239	9366144	31.28
49	Phthalic acid, di(2-propylpentyl) ester	$C_{24}H_{38}O_4$	390.556	22.239	9366144	31.28
50	Erucic acid	$C_{22}H_{42}O_2$	338.567	22.323	1022258	3.41

(MF) Molecular Formula, (MW) Molecular Weight, (RT) Retention Time

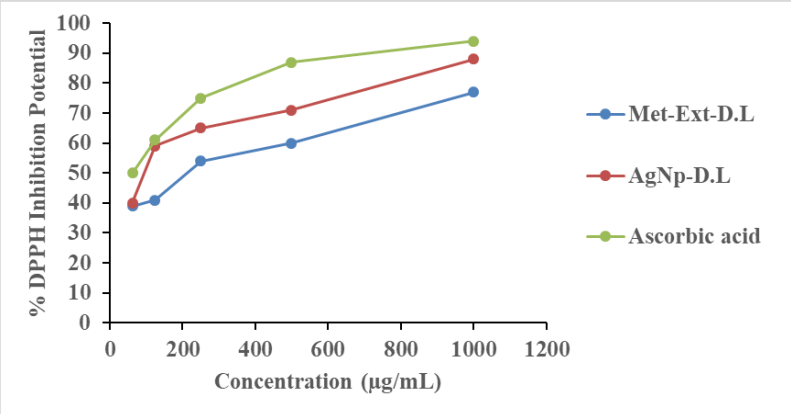

Figure S1. *% DPPH free radical scavenging potential of AgNPs and Met-Ext of D. longifolia leaves at different concentrations*

http://www.aloki.hu ● ISSN 1589 1623 (Print) ● ISSN 1785 0037 (Online)
DOI: http://dx.doi.org/10.15666/aeer/2304_67876815

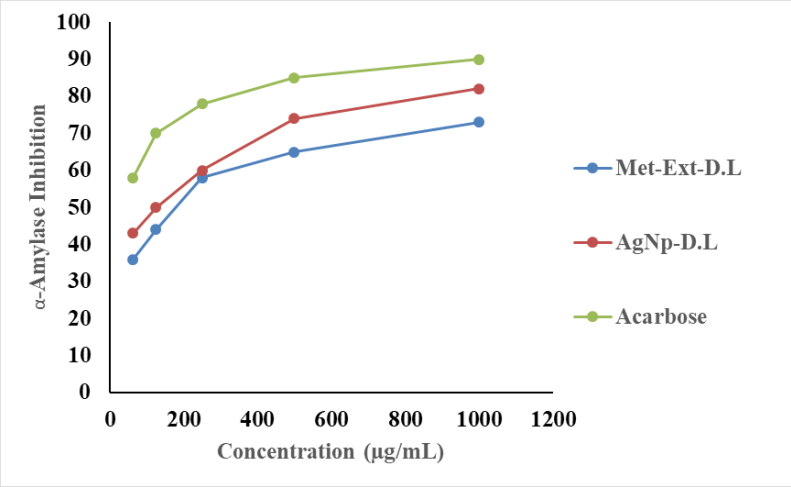

Figure S2. *% α-amylase inhibition potential of AgNPs and Met-Ext of D. longifolia at various concentrations*

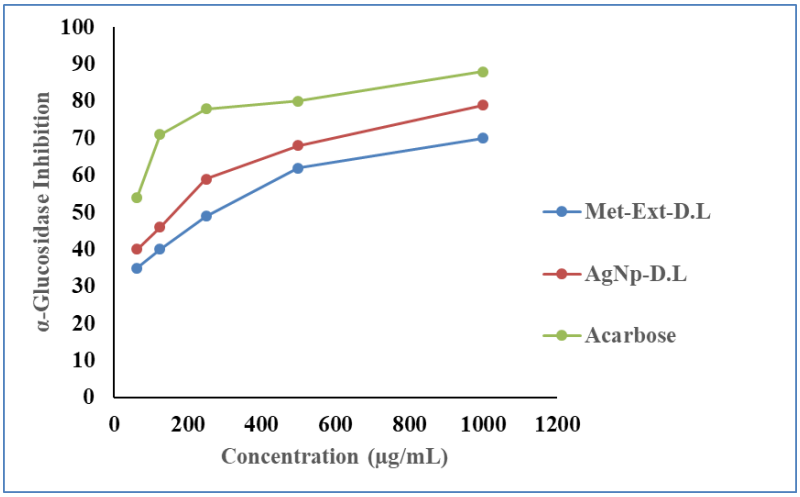

Figure S3. *% α-glucosidase inhibition potential of AgNPs and Met-Ext of D. longifolia at various concentrations*

http://www.aloki.hu ● ISSN 1589 1623 (Print) ● ISSN 1785 0037 (Online)
DOI: http://dx.doi.org/10.15666/aeer/2304_67876815